Electroneutral Polymer Nanodiscs Enable Interference-Free Probing of Membrane Proteins in a Lipid-Bilayer Environment

David Glueck, Anne Grethen, Manabendra Das, Ogochukwu Patricia Mmeka, Eugenio Pérez Patallo, Annette Meister, Ritu Rajender, Stefan Kins, Markus Räschle, Julian Victor, Ci Chu, Manuel Etzkorn, Zoe Köck, Frank Bernhard, Jonathan Oyebamiji Babalola, Carolyn Vargas, and Sandro Keller*

Membrane proteins can be examined in near-native lipid-bilayer environments with the advent of polymer-encapsulated nanodiscs. These nanodiscs self-assemble directly from cellular membranes, allowing in vitro probing of membrane proteins with techniques that have previously been restricted to soluble or detergent-solubilized proteins. Often, however, the high charge densities of existing polymers obstruct bioanalytical and preparative techniques. Thus, the authors aim to fabricate electroneutral—yet water-soluble—polymer nanodiscs. By attaching a sulfobetaine group to the commercial polymers DIBMA and SMA(2:1), these polyanionic polymers are converted to the electroneutral maleimide derivatives, Sulfo-DIBMA and Sulfo-SMA(2:1). Sulfo-DIBMA and Sulfo-SMA(2:1) readily extract proteins and phospholipids from artificial and cellular membranes to form nanodiscs. Crucially, the electroneutral nanodiscs avert unspecific interactions, thereby enabling new insights into protein–lipid interactions through lab-on-a-chip detection and in vitro translation of membrane proteins. Finally, the authors create a library comprising thousands of human membrane proteins and use proteome profiling by mass spectrometry to show that protein complexes are preserved in electroneutral nanodiscs.

1. Introduction

Membrane proteins constitute ≈23% of the human proteome and account for over 60% of current drug targets.[1] Despite their evident importance in biology and medicine, membrane proteins are challenging to analyze in vitro because it is difficult to extract them from a lipid membrane gently; that is, without perturbing the protein's native structure and function. Over recent years, membrane mimics offering a lipid bilayer,[2] such as membrane-scaffold protein (MSP) nanodiscs,[3] have been used with great success. However, these methods also require conventional detergents in time-consuming and potentially deleterious initial steps.[4]

Overcoming these pitfalls, amphiphilic copolymers such as diisobutylene/maleic acid (DIBMA)[5] and styrene/maleic acid (SMA)[6] have emerged as alternatives to

D. Glueck, A. Grethen, M. Das, O. P. Mmeka, E. P. Patallo,
C. Vargas, S. Keller
Molecular Biophysics
Technische Universität Kaiserslautern (TUK)
Erwin-Schrödinger-Str. 13, 67663 Kaiserslautern, Germany
E-mail: sandro.keller@uni-graz.at
D. Glueck, C. Vargas, S. Keller
Biophysics, Institute of Molecular Biosciences (IMB)
NAWI Graz
University of Graz
Humboldtstr. 50/III, Graz 8010, Austria
D. Glueck, C. Vargas, S. Keller
Field of Excellence BioHealth
University of Graz
Graz, Austria

D. Glueck, C. Vargas, S. Keller
BioTechMed-Graz
Graz, Austria
O. P. Mmeka, J. O. Babalola
Department of Chemistry
University of Ibadan
Ibadan 200284, Nigeria
A. Meister
HALOmem and Institute of Biochemistry and Biotechnology
Martin Luther University Halle-Wittenberg
Kurt-Mothes-Str. 3a, 06120 Halle (Saale), Germany
R. Rajender, S. Kins
Human Biology
Technische Universität Kaiserslautern (TUK)
Erwin-Schrödinger-Str. 13, 67663 Kaiserslautern, Germany
M. Räschle
Molecular Genetics
Technische Universität Kaiserslautern (TUK)
Paul-Ehrlich-Str. 24, 67663 Kaiserslautern, Germany
J. Victor, C. Chu, M. Etzkorn
Institut für Physikalische Biologie
Heinrich-Heine-Universität Düsseldorf
Universitätsstr. 1, 40225 Düsseldorf, Germany

ADVANCED
SCIENCE NEWS
www.advancedsciencenews.com

NANO · MICRO
small
www.small-journal.com

conventional detergents for solubilizing, extracting, and purifying integral membrane proteins.[7,8] These polymers induce formation of nanodiscs composed of a lipid-bilayer patch surrounded by a polymer belt.[9–11] The proteins simply remain embedded in their native lipid-bilayer patch as part of the DIBMA or SMA nanodiscs, and detergents are not required.[12] Nonetheless, the high charge densities of both DIBMA and SMA lead to unspecific interactions with charged proteins and lipids. Such unspecific interactions interfere with labile protein–protein and protein–lipid interactions and also with enzymatic (especially ribosomal) activities.[13] Furthermore, they obstruct many preparative and analytical techniques, such as protein electrophoresis and cell-free protein translation.[4,14] Thus, creating electroneutral polymers for lipid-bilayer nanodiscs has become an attractive goal.

One approach toward electroneutrality has been to incorporate phosphocholine pendant groups into the zwitterionic copolymer zSMA, which was synthesized *de novo*.[15,16] While zSMA has shown promise for biological applications, the multistep nature of its synthesis has so far prevented its widespread use in membrane-protein applications. A considerably simpler synthetic approach was to modify commercially available SMA backbones with ionizable pendant groups. Although chemically straightforward, the resulting polymers are water-soluble only when they carry a net charge.[17] With this simplified approach in mind, we hypothesized that a sulfobetaine moiety would provide the desired electroneutrality without sacrificing solubility. Sulfobetaine is zwitterionic at biologically relevant pH values, so we reasoned that its polymer chains and nanodiscs should also be electroneutral. In addition, sulfobetaine is found in popular buffers (in particular, Good's buffers), attesting to its high water solubility and excellent biocompatibility.

Here, we present two new electroneutral—yet water-soluble—polymers, Sulfo-DIBMA and Sulfo-SMA(2:1), formed by attaching sulfobetaine to the commercially available polymers DIBMA and SMA(2:1), respectively. We show that the new polymers quantitatively solubilize phospholipid bilayers and extract proteins from cellular membranes to form electroneutral nanodiscs. The electroneutrality of the new nanodiscs allows charge-sensitive protein–lipid interactions to be reliably detected and quantified—for the first time—by the new lab-on-a-chip method, microfluidic diffusional sizing (MDS). The unique combination of electroneutral nanodiscs and MDS reveals protein–lipid interactions that are otherwise overshadowed by unspecific electrostatic effects in the case of charged nanodiscs. We further highlight the benefit of these electroneutral polymers for cell-free translation and in vitro folding of membrane proteins. Like MDS, cell-free protein translation has so far been incompatible with polymer-encapsulated nanodiscs because of interference due to unspecific electrostatic interactions. Moreover, we demonstrate that the proteins extracted by the sulfopolymers can be directly analyzed by electrophoresis with no need for prior polymer removal. We exploit these properties for creating soluble libraries comprising thousands of human membrane proteins embedded in a nanoscale lipid-bilayer environment that preserves the integrity of protein complexes and is amenable to proteome profiling by mass spectrometry.

2. Results

### 2.1. Design and Synthesis of Electroneutral Sulfobetaine Polymers

The sulfobetaine group was chosen for functionalization for three reasons: First, sulfobetaine is zwitterionic at biologically relevant pH values, so its polymer chains and nanodiscs remain electroneutral (sulfonic acid and quaternary ammonium groups have pK_a values of <0 and ≈10, respectively). Second, sulfobetaine is strongly hydrated and, therefore, highly water-soluble despite being electroneutral. Third, sulfobetaine is biocompatible; that is, inert toward biomolecules. We aimed to develop a simple, accessible procedure to functionalize commercially available polymers with sulfobetaine in high purity and at low cost. Therefore, the functionalization must be quantitative (to avoid the need for any postmodification sample clean-up), but also simple to monitor, ideally with infrared (IR) spectroscopy, a fast and robust analytical technique accessible to most laboratories. Finally, we sought a modular route that would potentially allow other zwitterionic pendant groups, fluorescence labels, or affinity tags to be attached.

To meet all of the above criteria, we used the following two-step modification protocol (**Figure 1**): In the first step, the anhydrides of DIBMA and SMA(2:1) were converted into their corresponding maleamidic acids by amidation with 3-(dimethylamino)-1-propylamine or 2-(dimethylamino)-ethylamine followed by temperature-induced ring-closing imidization in a quantitative one-pot setup. In the second step, the resulting dimethylaminoalkyl maleimide copolymers reacted with 1,3-propane sultone to afford the desired maleimide sulfobetaines, Sulfo-DIBMA (Figure 1A) and Sulfo-SMA(2:1) (Figure 1B), in quantitative yields, as confirmed by attenuated-total-reflection Fourier-transform IR and ^1H nuclear magnetic resonance (NMR) spectroscopy (Figure S1, Supporting Information). The mass-average molar masses of Sulfo-DIBMA and Sulfo-SMA(2:1) were 14.0 and 12.6 kDa, respectively, as measured by using size-exclusion chromatography (SEC) coupled to refractive-index detection (Figure S2, Supporting Information). These molar masses agree well with nominal expectations based on the molar masses of DIBMA and SMA(2:1).

2.2. Sulfo-DIBMA and Sulfo-SMA(2:1) Induce Self-Assembly of Well-Defined, Electroneutral Nanodiscs

We elucidated the ability of Sulfo-DIBMA to induce nanodisc formation by exposing unilamellar vesicles composed of the zwitterionic, saturated phospholipid 1,2-dimyristoyl-*sn*-glycero-3-phosphocholine (DMPC) to increasing concentrations of Sulfo-DIBMA. The formation of Sulfo-DIBMA/DMPC nanodiscs was monitored by measuring particle size with dynamic light scattering (DLS; **Figure 2**A). The hydrodynamic particle

Z. Köck, F. Bernhard
Centre for Biomolecular Magnetic Resonance
Institute for Biophysical Chemistry
Goethe University of Frankfurt/Main
Max-von-Laue-Str. 9, 60438 Frankfurt/Main, Germany
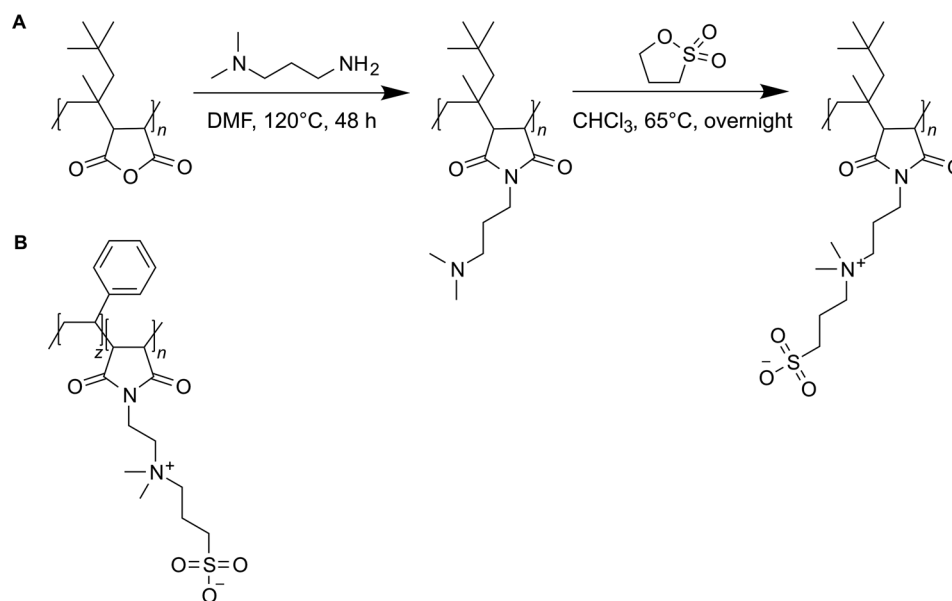
Figure 1. Synthetic route for the electroneutral sulfo-polymers. A) Sulfo-DIBMA formation from maleimide copolymer and 1,3-propane sultone. B) Sulfo-SMA(2:1) structure.

size initially increased to 215 nm at a polymer/lipid mass ratio of $m_p/m_l = 0.1$ (Figure 2A, down arrow) but then dropped steeply to $\approx$15 nm at $m_p/m_l = 0.5$ (Figure 2A, up arrow), finally flattening out to a constant value of $\approx$8 nm. These Sulfo-DIBMA nanodiscs were 2–4-fold smaller and more narrowly distributed than those prepared with unmodified DIBMA, as deduced from average particle sizes and peak widths, respectively, at given m_p/m_l values (Figure S3, Supporting Information).

Nanodisc formation was examined quantitatively with the aid of ^{31}P NMR spectroscopy (Figure 2B; and Figure S4, Supporting Information). In the absence of polymer, the signal from the large, slow-tumbling DMPC vesicles was broad beyond detection. Upon titration with polymer, we observed sharp, narrow peaks, which are characteristic of fast-tumbling particles. In the language of the three-stage model commonly invoked for lipid-solubilization titrations,[18] the first Sulfo-DIBMA nanodiscs formed at a saturating (SAT) surfactant/lipid mass ratio of $R_{SAT} = 0.038$, while solubilization (SOL) was complete at $R_{SOL} = 0.26$ (Figure S4, Supporting Information). This R_{SOL} value shows that equilibrium solubilization driven by Sulfo-DIBMA was threefold more efficient than for DIBMA ($R_{SOL} = 0.77$),[19] a finding that is consistent with the above DLS data (Figure 2A).

Measurements of ζ-potential confirmed the negligible surface charge, both on the bare Sulfo-DIBMA polymers and on the nanodiscs formed in mixtures with zwitterionic DMPC (Figure 2C). In stark contrast, polyanionic DIBMA and its nanodiscs displayed substantially negative ζ-potentials ranging from −15 to −20 mV. The size and morphology of the nanodiscs were examined by negative-stain transmission electron microscopy (TEM; Figure 2D). The nanodiscs were homogeneous, with a diameter of (11.5 ± 2.0) nm and a lipid-bilayer thickness of (4.9 ± 0.8) nm, as shown by face-on and edge-on views, respectively. These sizes are consistent with those measured by DLS (Figure 2A). In contrast with underivatized DIBMA, Sulfo-DIBMA efficiently solubilized the anionic, unsaturated,

long-chain phospholipid 1-palmitoyl-2-oleoyl-*sn*-glycero-3-phospho-(1′-*rac*-glycerol) (POPG; Figure 2E).

We obtained similar results for Sulfo-SMA(2:1) and the corresponding nanodiscs (Figure S5, Supporting Information). The efficiency of Sulfo-SMA(2:1) in solubilizing DMPC vesicles seen by DLS was similar to that of SMA(2:1), which in turn is more efficient than DIBMA. We can conclude that Sulfo-DIBMA and Sulfo-SMA(2:1) form well-defined, electroneutral nanodiscs. Also, compared with DIBMA and SMA(2:1), the Sulfo-polymers more efficiently solubilize membranes rich in anionic lipids, as found in most prokaryotes and the intracellular environment of eukaryotes. This enhanced membrane-solubilizing ability is likely due to the electroneutrality imparted by the zwitterionic sulfobetaine group attached to an uncharged maleimide backbone.

2.3. Electroneutral Nanodiscs are Stable toward Changes in pH and Ion Concentration

To serve as robust membrane mimetics, nanodiscs must be colloidally stable across the physiologically most relevant pH range as well as in the presence of functionally important divalent cations. Both factors pose serious limitations to existing, polyanionic polymers, which precipitate upon charge neutralization by protonation or cation binding.[5,20] Thus, we monitored the formation of electroneutral Sulfo-DIBMA nanodiscs across the pH range of 6.5–8.3. Nanodiscs formed at a constant Sulfo-DIBMA/DMPC mass ratio regardless of pH (**Figure 3**A), attesting to a robust, pH-independent solubilization efficiency. By contrast, both DIBMA and SMA(2:1) suffer from decreasing lipid-solubilizing power with increasing pH.[19,21] Moreover, Sulfo-DIBMA nanodiscs were colloidally stable in the presence of Mg^{2+} or Ca^{2+} concentrations as high as 80 mM, which manifested both in a clear visual appearance (Figure 3B) and
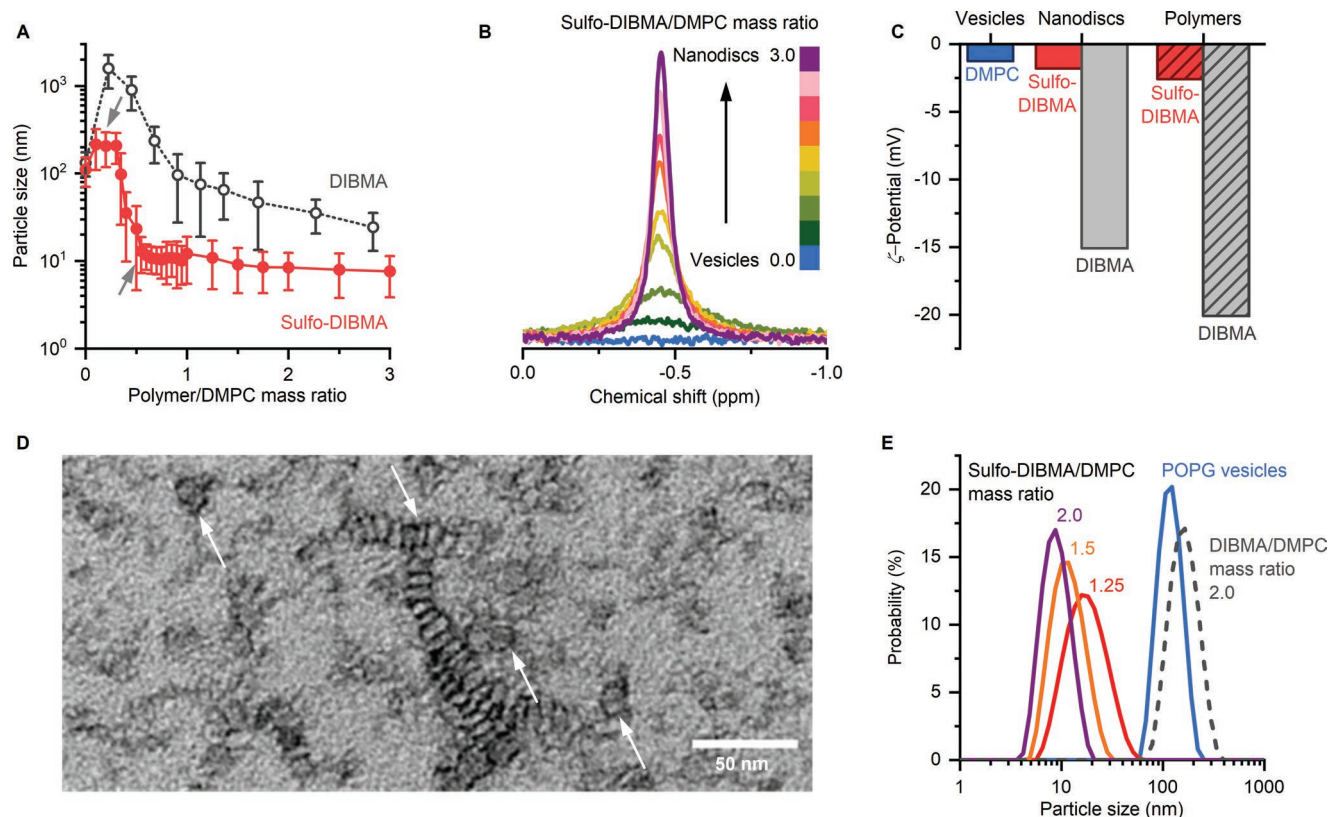
Figure 2. Solubilization of lipid vesicles and nanodisc formation by Sulfo-DIBMA. A) z-Average particle size derived from DLS as a function of polymer/lipid mass ratio. The graph shows that the electroneutral derivative Sulfo-DIBMA formed smaller, more narrowly distributed nanodiscs than unmodified DIBMA. Arrows indicate the onset (down arrow) and completion (up arrow) of nanodisc formation. Vertical bars are not error bars but indicate the peak width of the particle-size distribution as given by $\sigma = \sqrt{PDI}\, z$, with PDI being the polydispersity index and z the z-average particle size. B) ^{31}P NMR spectra of 4.0 mg mL^{-1} DMPC in the presence of increasing Sulfo-DIBMA concentrations. C) ζ-Potentials of polymers, polymer-encapsulated DMPC nanodiscs, and DMPC vesicles in the presence of 50 mM Tris, 100 mM NaCl, pH 7.4. The graph shows that sulfobetaine modification dramatically reduced the surface charge of both the polymer and the nanodiscs. D) Negative-stain TEM images of 0.01 mg mL^{-1} nanodiscs at $m_{\text{Sulfo-DIBMA}}/m_{\text{DMPC}} = 1.0$ prepared on a carbon-coated copper grid. Arrows indicate representative face-on (up arrows) and edge-on (down arrows) nanodisc views. E) Intensity-weighted particle-size distributions of aqueous mixtures of Sulfo-DIBMA or DIBMA and the anionic, unsaturated phospholipid POPG at various polymer/lipid mass ratios, as obtained from DLS. The particle size approached 10 nm for Sulfo-DIBMA, indicating nanodisc formation, whereas DIBMA failed to solubilize POPG vesicles. All experiments were carried out at 50 mM Tris, 200 mM NaCl, pH 7.4 unless noted otherwise.

in constant hydrodynamic particle-size distributions (Figure S6, Supporting Information). Sulfo-SMA(2:1) was similarly stable (Figure S7, Supporting Information), whereas DIBMA and SMA(2:1) precipitated at considerably lower divalent-cation concentrations (≈40 and ≈5 mM, respectively) (Figure 3B).[5,20]

2.4. Lipid-Bilayer Architecture and Packing are Preserved in Sulfo-DIBMA and Sulfo-SMA(2:1) Nanodiscs

To gauge the effect of the new polymers on phospholipid packing, we used differential scanning calorimetry (DSC) to monitor the temperature-dependent behavior of DMPC in nanodiscs formed by Sulfo-DIBMA (Figure 3C,D). With increasing temperature, DMPC vesicles exhibited the expected gel-to-fluid transition at $T_m = 24$ °C, which was reflected in a sharp peak in the isobaric heat capacity (Figure 3C). This peak broadened on addition of Sulfo-DIBMA (Figure 3C), confirming that nanoscale bilayer patches had formed with a much smaller cooperative unit than in vesicular bilayers.[22,23] This is in

line both with theoretical expectations[24] as well as with previous observations on MSP nanodiscs,[22] where it was also reported that saturated phospholipids exhibit broader melting transitions when embedded in a nanoscale bilayer. In spite of this broadening, the phase-transition temperature of DMPC increased only slightly and monotonically as Sulfo-DIBMA was added, indicating that the polymer exerts moderate lateral pressure on the encapsulated lipid-bilayer patch. Upon addition of DIBMA, by contrast, T_m initially increased more drastically before decreasing again, suggesting major alterations in lateral pressure with varying polymer/lipid ratio (Figure 3D). Thus, the already small influence of DIBMA on the T_m of DMPC was further mitigated in the case of Sulfo-DIBMA. For Sulfo-SMA(2:1) nanodiscs, T_m also slightly increased, whereas SMA(2:1) caused a drastic decrease in T_m (Figure S8, Supporting Information). In conclusion, the observation that the T_m of DMPC was hardly affected by Sulfo-DIBMA or Sulfo-SMA(2:1) indicates that these electroneutral polymers only mildly affect the acyl-chain packing of the phospholipids that they encapsulate. This contrasts sharply with the pronounced

**ADVANCED
SCIENCE NEWS**

www.advancedsciencenews.com

NANO · MICRO

small

www.small-journal.com
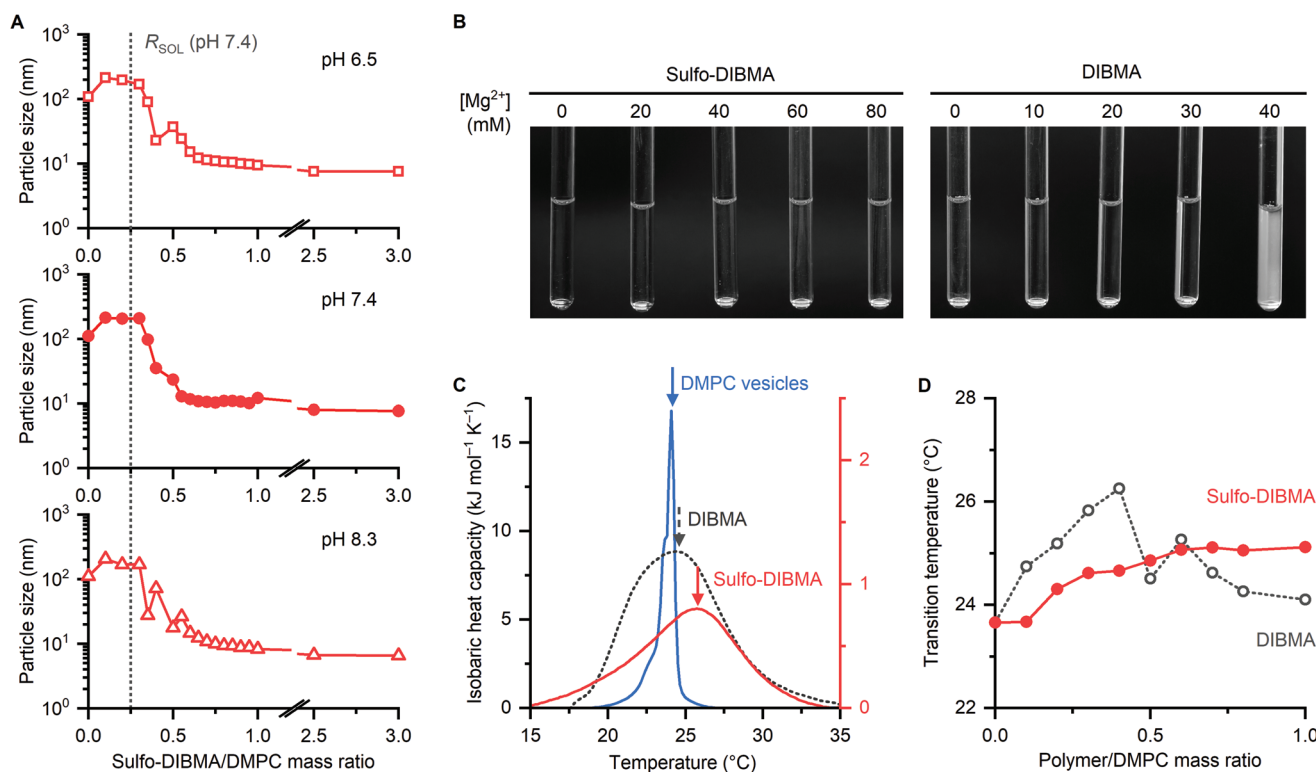
Figure 3. Stability toward pH and divalent cations as well as thermotropic phase transitions in Sulfo-DIBMA nanodiscs. A) z-Average sizes as functions of Sulfo-DIBMA/DMPC mass ratio at different pH values. The vertical dotted line denotes R_{SOL} for Sulfo-DIBMA-mediated DMPC solubilization at pH 7.4. Solubilization efficiencies and particle sizes were unaffected by pH. B) Visual appearance of Sulfo-DIBMA and DIBMA nanodiscs at $m_{polymer}/m_{DMPC} = 1.5$ in the presence of increasing Mg^{2+} concentrations. C) DSC thermograms showing excess molar isobaric heat capacities of 4.0 mg mL^{-1} DMPC vesicles (left γ-axis) and Sulfo-DIBMA or DIBMA nanodiscs (right γ-axis) at $m_{polymer}/m_{DMPC} = 1.0$. Vertical arrows indicate the gel-to-fluid phase transition temperature for each membrane system. D) Gel-to-fluid phase-transition temperatures of 4 mg mL^{-1} DMPC at various polymer/lipid mass ratios. Experiments were carried out at 50 mM Tris, 200 mM NaCl, pH 7.4 unless noted otherwise.

perturbation of the lipid bilayer caused by polyanionic SMA polymers in particular.[5,21,25]

2.5. Charge-Sensitive Protein–Lipid Interactions can be Probed Without Interference

Charge-sensitive protein–lipid interactions are involved in many physiologically relevant but barely understood processes. For example, the binding and (mis)folding of proteins on lipid membranes are thought to underlie amyloid-plaque formation in neurodegenerative diseases.[26] Therefore, understanding protein–lipid interactions may have important implications for biology and medicine. However, these interactions cannot be studied with existing polymer nanodiscs (such as those based on DIBMA and SMA) because their polyionic polymer chains interfere with such charge-sensitive interactions. We assessed the usefulness of Sulfo-DIBMA and Sulfo-SMA(2:1) polymers for probing protein–lipid interactions by means of microfluidic diffusional sizing (MDS), a recent lab-on-a-chip technique that requires only microliter volumes of sample.[27–31] MDS can detect binding of proteins to lipid bilayers by measuring changes in the effective hydrodynamic size of the protein upon membrane binding. Since vesicles tend to exceed the hydrodynamic-size range applicable for MDS, smaller lipid-bilayer

nanoparticles are needed for analyzing protein–lipid interactions. Hence, Sulfo-DIBMA and Sulfo-SMA(2:1) nanodiscs are ideal candidates for this kind of assay.

To assess which polymers are able to probe charge-sensitive protein–lipid interactions, we first studied the membrane interactions of α-synuclein, a protein that plays a pivotal role in neurodegenerative diseases.[32] Physiologically, this water-soluble protein binds to presynaptic vesicles, which presumably aids synaptic release.[32] α-synuclein has a high affinity to anionic lipids, whereas interactions with zwitterionic lipids are weak.[33] Consequently, lipid-specific binding modes, predominantly those involving formation of amphipathic α-helices, have been detected using liposomes[34,35] and MSP nanodiscs.[36] Due to its well-established lipid-binding properties, α-synuclein here served as a positive control for our assay (**Figure 4**A). Thus, we titrated α-synuclein with nanodiscs formed from the different polymers and harboring either zwitterionic DMPC or anionic DMPG (1,2-dimyristoyl-sn-glycero-3-phospho-(1'-rac-glycerol)). Upon titration with anionic DMPG encapsulated by either Sulfo-DIBMA or Sulfo-SMA(2:1), the hydrodynamic size of α-synuclein increased from 7 nm to about 16 nm, which is consistent with binding of the protein to these nanodiscs (Figure 4B). Upon titration with zwitterionic DMPC encapsulated by either of the two electroneutral polymers, however, α-synuclein did not bind to the nanodiscs, as evidenced by its
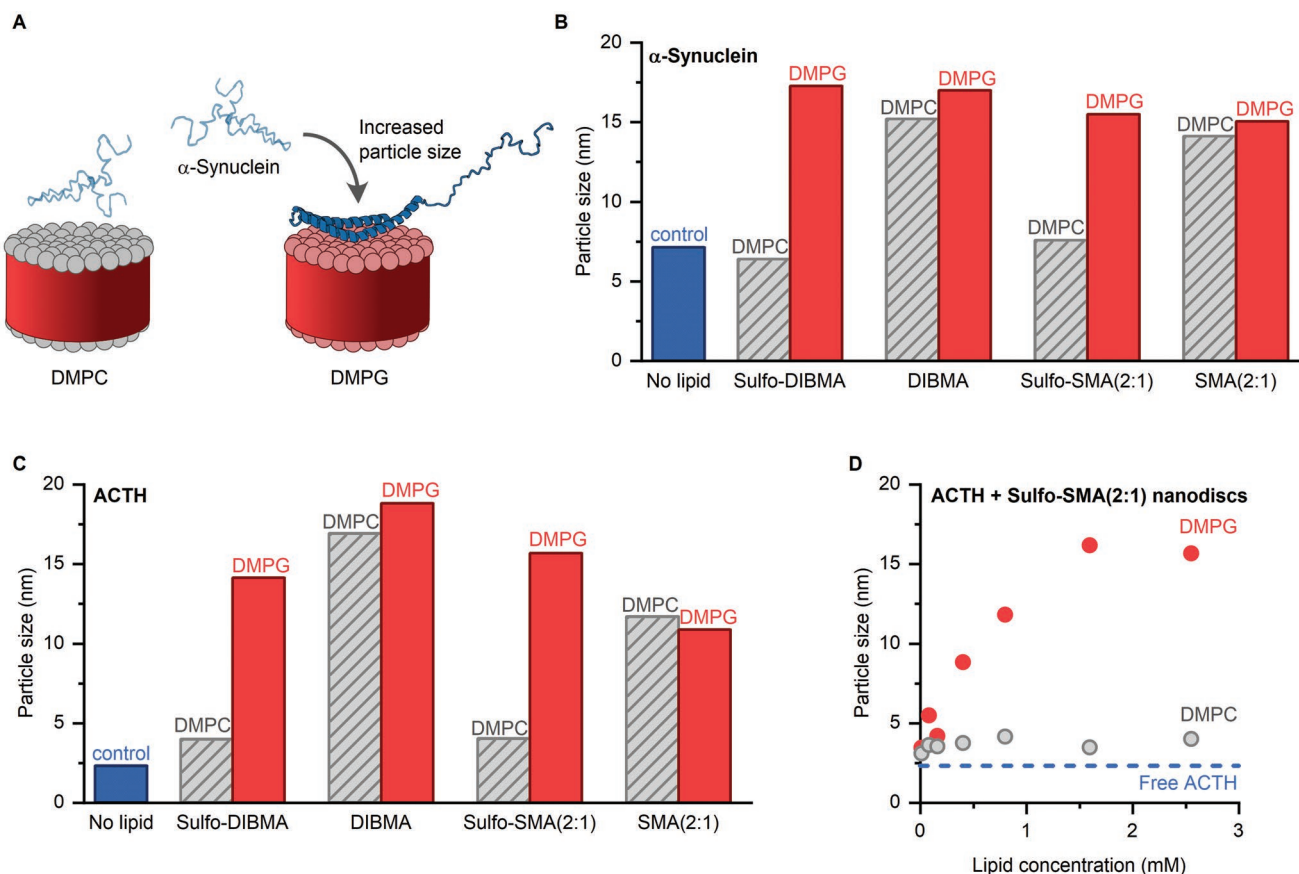
Figure 4. Electroneutral nanodiscs enable probing of lipid-specific protein–lipid interactions via MDS. A) Schematic showing that α-synuclein selectively binds to and folds at anionic membrane surfaces, such as DMPG, resulting in a protein–nanodisc assembly with increased hydrodynamic size.[40] By contrast, α-synuclein should not interact with nanodiscs having electroneutral surfaces, such as DMPC. B) Particle size of α-synuclein in the absence and presence of DMPC or DMPG nanodiscs formed from Sulfo-DIBMA, DIBMA, Sulfo-SMA(2:1), or SMA(2:1). C) Particle size of ACTH in the absence and presence of DMPC or DMPG nanodiscs formed from Sulfo-DIBMA, DIBMA, Sulfo-SMA(2:1), or SMA(2:1). ACTH showed strong selectivity for DMPG lipids in Sulfo-DIBMA and Sulfo-SMA(2:1) nanodiscs but not in nanodiscs made from negatively charged DIBMA or SMA(2:1). D) Particle size of ACTH upon titration with Sulfo-SMA(2:1) nanodiscs containing zwitterionic DMPC or anionic DMPG.

unchanged hydrodynamic size. In stark contrast, titration with nanodiscs formed from polyanionic DIBMA or SMA always revealed binding of α-synuclein to the nanodiscs irrespective of the charge of the encapsulated lipid, obscuring any lipid-specific effects. Thus, our data clearly demonstrate that the expected lipid specificity of this interaction is detected only for nanodiscs formed from electroneutral Sulfo-DIBMA or Sulfo-SMA.
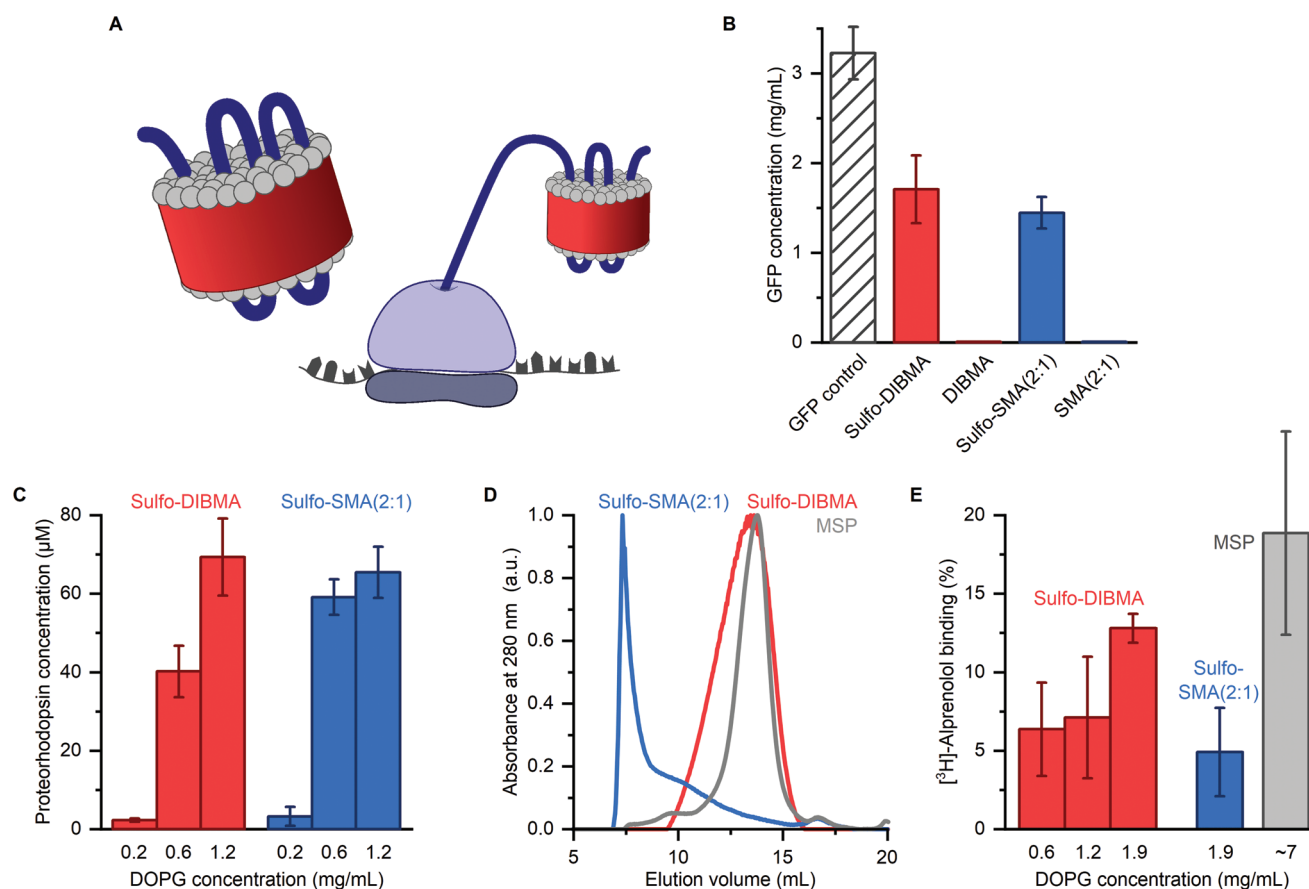
Following our positive control, we examined the less-well-characterized binding of the peptidic adrenocorticotropic hormone (ACTH) to DMPC and DMPG nanodiscs.[37] As for other secretory peptides, binding to anionic lipids is thought to facilitate directed intracellular transport by vesicles.[38] Indeed, we observed that ACTH strongly preferred anionic DMPG over zwitterionic DMPC in both Sulfo-SMA(2:1) and Sulfo-DIBMA nanodiscs (Figure 4C,D). Here again, this lipid specificity was lost when ACTH was exposed to nanodiscs encapsulated by polyanionic SMA(2:1) or DIBMA, which gave rise to unspecific interactions irrespective of the chemical nature of the lipid constituent (Figure 4C). With the aid of Sulfo-DIBMA nanodiscs, we probed the charge-sensitive membrane interactions of ACTH over several orders of magnitude of lipid concentrations

(Figure 4D). Thus, MDS measurements enabled us to reliably detect even the rather weak interaction of ACTH with DMPG lipids.

Finally, we used monomeric guanine nucleotide-binding protein subunit β1 (GB1) as a negative control. Because GB1 in its monomeric form does not interact with DMPC or DMPG, the protein should be inert toward Sulfo-nanodiscs regardless of their lipid constituents.[39] As expected, GB1 showed no increase in size in the presence of Sulfo-SMA(2:1) nanodiscs (Figure S9, Supporting Information). Taken together, these three examples demonstrate that the new, electroneutral polymers do not interfere with charge-sensitive protein–lipid interactions and—for the first time—enable sensitive membrane-interaction assays in a microfluidic format.

2.6. Electroneutral Nanodiscs Support Cell-Free Membrane-Protein Synthesis

Cell-free synthesis of proteins is a key tool for investigating unknown gene products, especially for proteins that are

**ADVANCED
SCIENCE NEWS**

www.advancedsciencenews.com

**NANO · MICRO
small**

www.small-journal.com

Figure 5. Cell-free synthesis of membrane proteins into electroneutral polymer nanodiscs. A) Schematic showing membrane proteins being translated and directly inserted into nanodiscs. B) Tolerance of the in vitro translation system toward polymers. Sulfo-DIBMA and Sulfo-SMA(2:1) enabled the synthesis of folded GFP, whereas the unmodified polymers DIBMA and SMA(2:1) completely inhibited it. C) Yields of proteorhodopsin synthesized in the presence of increasing concentrations of Sulfo-DIBMA or Sulfo-SMA(2:1) nanodiscs. D) SEC elution profiles of proteorhodopsin synthesized in the presence of nanodiscs at a lipid concentration of 1.2 mg mL^{-1} (1.55 mM) and of a proteorhodopsin reference synthesized in the presence of MSP1E3D1 nanodiscs. E) Binding of [^{3}H]-alprenolol to Tβ1AR/GFP, as quantified by a filter binding assay. Shown is the percentage of Tβ1AR/GFP that can bind the ligand. Error bars indicate standard deviations of experimental triplicates.

unstable in, or toxic to, living hosts.[41] However, this technique is not compatible with existing polymer nanodiscs because negatively charged polymers adversely affect the concentration of free Mg^{2+}, which needs to be tightly controlled during cell-free protein translation.[42,43] Since we have now shown that Sulfo-polymer nanodiscs do not interact with Mg^{2+} (Figure 3B) and do not interfere with charge-sensitive protein–lipid interactions (Figure 4), we reasoned that Sulfo-DIBMA and Sulfo-SMA(2:1) may be suitable for the cotranslational insertion of membrane proteins synthesized by cell-free translation (**Figure 5**A).

We first assessed the synthesis of green fluorescent protein (GFP) as a soluble model protein (Figure 5B). Electroneutral Sulfo-DIBMA and Sulfo-SMA(2:1) nanodiscs clearly enabled cell-free synthesis, allowing translation of GFP at about half-maximal efficiency (1.7 and 1.5 mg mL^{-1}, respectively) relative to a positive control without membrane mimetics (3.2 mg mL^{-1}). By contrast, polyanionic DIBMA and SMA(2:1) essentially prevented cell-free synthesis, affording negligible concentrations of GFP (≈0.006 mg mL^{-1} for both).

To test whether the new nanodiscs would support the in vitro folding of membrane proteins during cell-free translation,

we turned to the light-gated proton pump proteorhodopsin. Cell-free production of proteorhodopsin was quantified over increasing nanodisc concentrations (Figure 5C).[44] With Sulfo-DIBMA or Sulfo-SMA(2:1) nanodiscs containing 1,2-dioleoyl-*sn*-glycero-3-phospho-(1′-*rac*-glycerol) (DOPG), we achieved a proteorhodopsin concentration of >65 μM at the highest lipid concentration tested (1.2 mg mL^{-1}, corresponding to 1.6 mM DOPG). Proteorhodopsin-containing nanodiscs were then affinity-purified by exploiting the C-terminal strep-tag attached to the protein. Subsequent SEC revealed that proteorhodopsin in Sulfo-DIBMA nanodiscs eluted as a single peak. This result is comparable to that observed for proteorhodopsin embedded in nanodiscs encapsulated by MSP (Figure 5D). By contrast, proteorhodopsin/Sulfo-SMA(2:1) samples eluted predominantly in the void peak, indicating the presence of particles much larger than individual nanodiscs. These observations suggest that aliphatic Sulfo-DIBMA is more suitable than aromatic Sulfo-SMA(2:1) for producing homogeneous lipid-bilayer particles that contain well-folded membrane proteins.

Finally, we investigated a representative of the pharmacologically highly relevant class of G-protein-coupled receptors

**ADVANCED
SCIENCE NEWS**
www.advancedsciencenews.com

**NANO · MICRO
small**
www.small-journal.com

(GPCRs), the turkey β1-adrenergic receptor (Tβ1AR). We synthesized a thermostabilized, GFP-coupled variant of Tβ1AR in the presence of increasing concentrations of polymer-encapsulated nanodiscs (Figure 5E).[45] We then assessed the functional folding of the Tβ1AR/GFP fusion construct directly in the cell-free reaction mixture by radio-ligand binding of the specific antagonist [3H]-alprenolol.[45] As gauged by the fraction of ligand binding, the yield of active, binding-competent Tβ1AR in the presence of Sulfo-DIBMA nanodiscs containing 1.9 mg mL^{-1} (2.4 mM) lipid amounted to ≈13%. By comparison, the yield of active Tβ1AR in the presence of MSP nanodiscs containing ≈7 mg mL^{-1} (≈9 mM) lipid was ≈18% (Figure 5E). Thus, we obtained similar yields of functional receptors within Sulfo-DIBMA nanodiscs, which, unlike MSP nanodiscs, can be produced rapidly without any detergent. Therefore, Sulfo-DIBMA enables screening of more experimental conditions with the same nanodisc batch, in higher quantities, and at significantly lower cost than MSP nanodiscs. With Sulfo-SMA(2:1) nanodiscs, the yield of active receptor was reduced to ≈5%, underlining the above conclusion that Sulfo-DIBMA is the preferred choice for the in vitro translation and lipid-bilayer insertion of natively folded membrane proteins.

2.7. New Polymers form Nanodisc Libraries Reflecting the Human Membrane Proteome

One of the decisive advantages of polymer-based nanodiscs over other lipid-bilayer membrane mimetics—including MSP nanodiscs—is the ability of polymers to directly extract proteins from cellular membranes. To assess whether electroneutral Sulfo-DIBMA would be useful for this purpose, we created soluble libraries of the human membrane proteome from HeLa cells (**Figure 6**A). Sodium dodecyl sulfate polyacrylamide gel electrophoresis (SDS-PAGE) of soluble sample fractions revealed that Sulfo-DIBMA successfully extracted a large number of membrane proteins of vastly different sizes, including proteins larger than 150 kDa (Figure 6B). Overall, Sulfo-DIBMA extracted 25% of the entire membrane-protein mass even at a polymer concentration as low as 4 mg mL^{-1} or 0.4% w/v (Figure 6C); that is, a substantially lower concentration than what is commonly used for extracting membrane proteins with amphiphilic polymers (25 mg mL^{-1} or 2.5% w/v).[4] Polyanionic DIBMA and the conventional detergent n-dodecyl-β-D-maltopyranoside (DDM) extracted about twice as much total protein mass as Sulfo-DIBMA. While DDM does not preserve a bilayer environment, DIBMA is highly negatively charged, which can reduce the stability of extracted membrane proteins (see below).

To obtain deeper insights into the native membrane proteome afforded by Sulfo-DIBMA, we first fractionated the nanodisc library obtained from whole-cell HeLa extraction by means of SEC. We then analyzed each fraction by liquid chromatography coupled to tandem mass spectrometry (LC-MS/MS). In total, we identified 2436 proteins in the Sulfo-DIBMA nanodisc library, 1280 of which are classified by the keyword "membrane" in the gene-ontology database. This amounts to ≈50% of the previously determined HeLa membrane proteome, which was pooled from multiple protein-extraction methods using much harsher, denaturing conditions.[46,47] Of note, the

entire Sulfo-DIBMA nanodiscs library eluted within the resolution range of the SEC column (20–600 kDa; Figure 6D), indicating that all extracted membrane proteins remained stably inserted into their nanoscale lipid-bilayer environment without aggregating, which is testament to our gentler extraction method. Sulfo-SMA(2:1) behaved similar to Sulfo-DIBMA, in that it yielded a relatively narrow chromatogram typical of well-folded and colloidally stable membrane proteins (Figure S10, Supporting Information). This is in sharp contrast with DIBMA nanodiscs, which spanned a much broader size range (100–3000 kDa) and displayed a substantial void peak indicative of protein aggregates (Figure 6E). Remarkably, this is in line with DLS data, where Sulfo-DIBMA produces smaller particles with narrower size distributions than its anionic counterpart (Figure 2A). Thus, the effects of the polymer on nanodisc size and lipid solubilization correlate with its effects on the extraction of proteins from complex, cellular membranes. As expected from the known bioinert properties of the sulfobetaine group,[48] we found no evidence of unspecific binding between soluble proteins and sulfo-nanodiscs. Neither the SEC chromatogram (Figure 6D,E) nor the MS elution profiles (Figure S11, Supporting Information) indicate the presence of protein aggregates, which is in line with our MDS data (Figure 4B,C). In conclusion, we have shown that the new, electroneutral polymers Sulfo-DIBMA and Sulfo-SMA(2:1) can be used to generate soluble libraries comprising thousands of human membrane proteins. These proteins remain surrounded by their endogenous lipids in a bilayer that is not perturbed by unspecific electrostatic effects or aggregation.

2.7.1. Membrane–Protein Complexes are Preserved in Nanodisc Libraries

After demonstrating the ability of the new polymers to directly extract entire membrane proteomes into well-defined lipid-bilayer nanodisc libraries, we zoomed in on four structurally and functionally diverse proteins residing in different cellular membranes. To this end, we focused on the SEC elution profiles of these four proteins taken from a comprehensive proteomics dataset (provided as the Supporting Information). This dataset was obtained by analyzing 30 SEC fractions of the entire nanodisc library (Figure 6D) with the aid of LC-MS/MS. Thus, we generated a global map of protein elution profiles, showing that the vast majority of extracted membrane proteins were found in single, well-defined peaks (Figure S11, Supporting Information).

For all proteins studied in the following section, the elution profile peaked at an apparent molecular weight 3–5 times the nominal molecular weight of the bare protein constituents. We observed this trend across the whole membrane proteome, where the median of individual protein sizes increased 3.3-fold (Figure S12, Supporting Information). The median of soluble-protein molecular weights, by contrast, increased only 1.7-fold. This is consistent with the lipid-bilayer patch and polymer belt contributing to the total molecular weight of nanodisc-embedded proteins in roughly proportional fashion.

Single-Pass α-Helical Membrane Protein: Cytochrome P450 reductase (CPR) is found in the membrane of the smooth
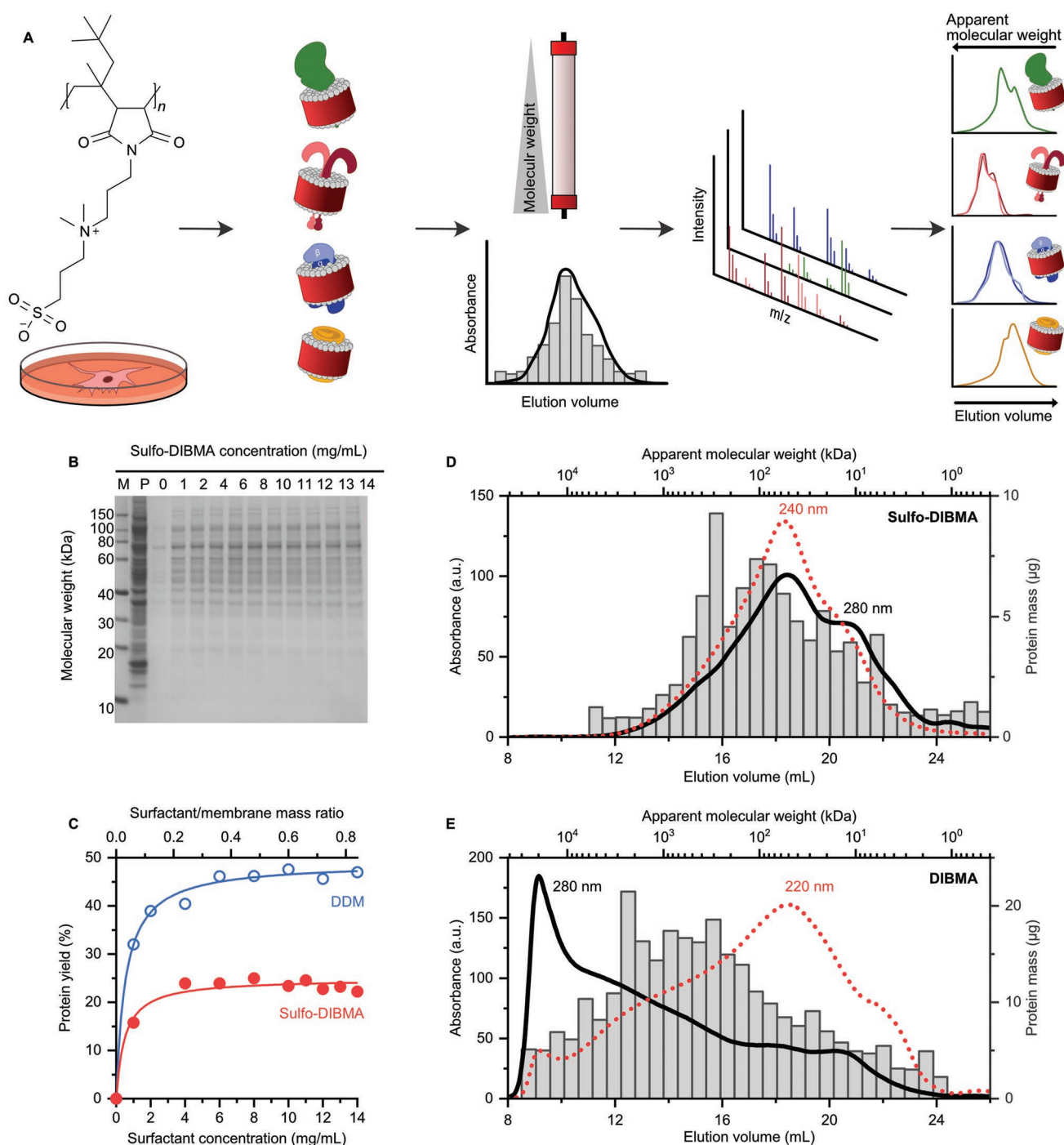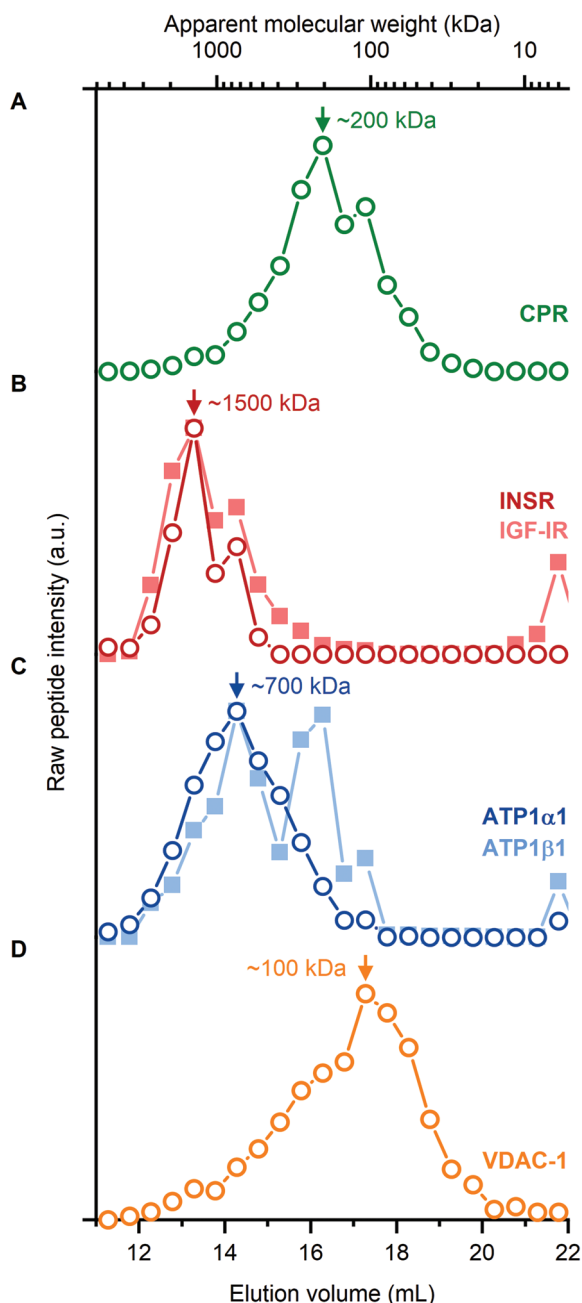
Figure 6. Extraction of membrane proteins from human cells using Sulfo-DIBMA. A) Workflow of membrane-proteome profiling with nanodisc-embedded proteins. For further details, see the Experimental Section. B) SDS-PAGE showing membrane proteins extracted from HeLa cells by increasing Sulfo-DIBMA concentrations after 12 h of incubation at 4 °C. Low-molecular-weight proteins gave rise to faint bands because of the rather low overall protein concentration and because these proteins generally bind less Coomassie stain. C) Overall yields of extracted membrane proteins as functions of polymer or detergent concentration as determined by a BCA (bicinchoninic acid) protein assay. D) SEC elution profiles of whole-cell extracts obtained by subjecting HeLa cells to 12 mg mL^{-1} Sulfo-DIBMA. E) SEC elution profiles of HeLa whole-cell extracts using 12 mg mL^{-1} DIBMA; axes as in panel (C). Protein extraction and SEC experiments were carried out at 50 mM Tris, 150 mM NaCl, pH 7.4.

endoplasmic reticulum, to which it is anchored through a single transmembrane helix.[49] CPR has previously been investigated in MSP nanodiscs. For that purpose, however, the protein had to be isolated with the harsh detergent Triton X-100, which displaced its native lipid environment before it was reconstituted into an artificial lipid bilayer.[50] Here, we demonstrate

Figure 7. SEC elution profiles of HeLa membrane proteins in native nanodisc libraries as determined by LC-MS/MS. A) CPR: NADPH/cytochrome P450 reductase; B) INSR: insulin receptor; IGF-IR: insulin-like growth factor 1 receptor; C) ATP1α/β1: α/β subunits of Na⁺/K⁺ ATPase; D) VDAC-1: voltage-dependent anion channel 1.

two proteins both have molecular weights around 310 kDa.[51] As expected for a mixture of homo- and heterodimers of virtually the same size, INSR and IGF-IR coeluted with high correlation, each showing a peak at ≈1500 kDa (Figure 7B).

Noncovalent Membrane–Protein Complex: The Na⁺/K⁺ ATPase (ATP1) is a heterotrimeric membrane-protein complex crucial for maintaining an electrochemical potential difference across the plasma membrane.[52] Importantly, the α- and β-subunits of this complex coeluted, showing a single peak at ≈700 kDa (Figure 7C), even though their molecular weights differ substantially (α- and β-subunits are 113 and 35 kDa, respectively). By contrast, the γ-subunit consists of a single transmembrane helix. Such small, hydrophobic peptides often cannot be detected by mass spectrometry, which was also the case here. Nonetheless, the excellent correlation between the elution profiles of the α- and β-subunits strongly indicates that Sulfo-DIBMA extracted the intact complex from HeLa cells, retaining the native subunit composition in the soluble membrane-protein library. In addition, the β-subunit eluted in a second peak at ≈200 kDa, which indicates a protein population not associated with the α-subunit. Biphasic elution profiles indicate protein states without or with different binding partners and have previously been observed in SEC/MS profiling studies.[53] This would render the Na⁺/K⁺ ATPase β-subunit a suitable protein for targeted protein–protein interaction studies. A case like this highlights the strength of SEC/MS profiling of native membrane-protein libraries in lipid-bilayer nanodiscs, as this elution behavior was unveiled among thousands of other identified proteins.

Multipass β-Sheet Membrane Protein: The voltage-dependent anion channel 1 (VDAC-1) is an abundant β-barrel protein localized predominantly in the outer membrane of mitochondria. This protein, which has been implicated in Alzheimer's and Parkinson's disease,[54] occurs in monomeric, homodimeric, and homotrimeric forms.[55] Indeed, we observed a broad elution profile peaking at ≈100 kDa but with a pronounced shoulder on the left-hand side, indicative of oligomeric species (Figure 7D). These results demonstrate that β-barrel membrane proteins and, more broadly, the densely protein-packed inner mitochondrial membrane were efficiently extracted by Sulfo-DIBMA.

Taken together, these examples show that Sulfo-DIBMA can directly extract proteins of various sizes, folds, and oligomeric states from different cellular membranes to afford a soluble library of membrane proteins embedded in electroneutral lipid-bilayer nanodiscs. This library can then be probed by native SEC followed by LC-MS/MS to yield a profile of the membrane proteome without the need for labels or antibodies. In contrast with previous work relying on MSP nanodiscs,[56] native membrane-protein complexes can thus be observed in a nanoscale bilayer environment without being reconstituted, crucially preserving noncovalent protein interactions.

3. Discussion

Self-assembling polymer nanodiscs enable researchers to study membrane proteins under well-defined in vitro conditions without ever removing these often-labile proteins from

that native CPR can readily be extracted into electroneutral nanodiscs without being removed from its lipid-bilayer environment, as confirmed by a well-defined peak at ≈200 kDa (**Figure** 7A).

Covalent Dimers of Single-Pass Membrane Proteins: The insulin receptor (INSR) and the insulin-like growth-factor receptor (IGF-IR) are receptor tyrosine kinases that exist in the plasma membrane as covalently linked homo- and heterodimers. The

ADVANCED
SCIENCE NEWS
www.advancedsciencenews.com

NANO · MICRO

small

www.small-journal.com

a lipid bilayer. A severe limitation inherent to existing polymers, including the two dominating variants DIBMA and SMA, is that their high charge densities—usually needed for water solubility—interfere with important bioanalytical and preparative techniques. In this work, we have developed two new zwitterionic polymers, Sulfo-DIBMA and Sulfo-SMA(2:1), which extract membrane proteins directly from cellular membranes, along with surrounding lipids, to form lipid-bilayer nanodiscs. The electroneutrality of our nanodiscs was shown by ζ-potential measurements. Despite their electroneutrality, these native nanodiscs are highly water-soluble and colloidally stable across a broad range of pH and ionic strength values.

Moreover, because of that electroneutrality, Sulfo-DIBMA and Sulfo-SMA(2:1) do not interfere with charge-sensitive protein–lipid interactions. For many membrane proteins, the role of lipids in modulating protein structure and function is not yet well understood, and there is a need for new methods to analyze these fundamental interactions. We have presented here a range of proof-of-principle studies that detect and quantify protein–lipid interactions in the following ways:

- We used the new lab-on-a-chip method, microfluidic diffusional sizing (MDS), to detect binding of several proteins to lipid bilayers. In contrast with dynamic light scattering (DLS), MDS selectively records the hydrodynamic size of the target molecule, even for proteins at low concentrations in complex mixtures. Moreover, we showed that, for quantifying charge-dependent protein–lipid interactions, this technique was effective only with nanodiscs prepared from our electroneutral polymers, Sulfo-DIBMA and Sulfo-SMA(2:1). Analogous experiments performed with the polyanionic analogues DIBMA and SMA(2:1) failed to detect lipid specificity because these highly charged polymer chains result in unspecific interactions between proteins and polymers that overshadow charge-sensitive protein–lipid interactions.
- We synthesized functionally folded forms of several integral membrane proteins in a cell-free manner with our electroneutral nanodiscs prepared from Sulfo-DIBMA and Sulfo-SMA(2:1). This in vitro protein synthesis was enabled by the sulfo-polymers because they are inert toward divalent cations such as Mg^{2+}, an essential cofactor for protein translation. Cell-free protein synthesis has not been shown for any polymer-encapsulated lipid-bilayer membrane mimetic before, and we confirmed here that it is not possible with the polyanionic analogues DIBMA and SMA(2:1) because these negatively charged polymers compete with the translation machinery for Mg^{2+}.
- We used a combination of chromatography and mass spectrometry (MS) to show that our nanodiscs preserve delicate membrane-protein complexes and protein–protein interactions within nanoscale lipid bilayers. With this approach, we provide a proteome dataset comprising several thousand human membrane proteins embedded in a nanodisc library.
- We showed that, even for a method as simple and common as SDS-PAGE, Sulfo-DIBMA and Sulfo-SMA(2:1) provide substantial benefits, as the polymers do not need to be removed before gel electrophoresis to avoid unspecific background staining in the gel, in contrast with charged polymers.

From a more chemical perspective, the high water solubilities of Sulfo-DIBMA and Sulfo-SMA(2:1) set them apart from existing polymers, whose ionizable groups confer solubility only when carrying a net charge.[17] The only exception is zSMA,[15,16] which contains a phosphocholine group that makes it water-soluble also in its zwitterionic state. However, the expensive and laborious *de novo* synthesis of zSMA followed by multistep postpolymerization functionalization has meant that it is not readily accessible to the rapidly growing community of structural biologists, protein biochemists, and membrane biophysicists relying on polymer-encapsulated nanodiscs. By contrast, Sulfo-DIBMA and Sulfo-SMA(2:1) are easily obtained from commercially available polymer scaffolds on a multigram scale in high yields and purities. Consequently, ready-to-use electroneutral polymers are now widely accessible, even to laboratories lacking dedicated equipment for, or expertise in, *de novo* polymer synthesis.

We envisage that our synthetic strategy can easily be expanded; for example, to include other zwitterionic or even nonionic pendant groups and fluorescent labels or affinity tags for capturing and immobilizing nanodiscs. For example, the maleimide amines obtained in the first step (Figure 1A) could be further derivatized to form a carboxybetaine[57] by simply replacing the sultone with an activated carboxylic acid in the second step.

For future applications, we anticipate that using lab-on-a-chip technologies such as MDS to investigate libraries of membrane proteins stably embedded in lipid-bilayer nanodiscs will be a powerful tool for monitoring protein–protein interactions under near-native conditions. For instance, the interactions between a fluorescent antibody and its membrane-bound antigen might be identified and quantified without needing to purify or remove the antigen from its lipid-bilayer environment. Such interaction assays have previously been restricted to water-soluble proteins[58] but now can be extended to membrane proteins—from any cellular compartment—embedded in electroneutral lipid-bilayer nanodiscs.

4. Conclusions

The electroneutral polymers introduced herein offer considerable advantages for membrane-protein research because they significantly extend the range of bioanalytical and preparative methods compatible with lipid-bilayer nanodiscs. Sulfo-DIBMA and Sulfo-SMA(2:1) can be readily obtained by a simple modification of commercial polyanionic precursors, allowing their low-cost and straightforward production in nonspecialized laboratories. Electroneutral polymer nanodiscs can then self-assemble directly from cellular membranes, enabling embedded proteins to be probed in vitro without ever being removed from their lipid-bilayer environment.

5. Experimental Section

Materials: DMPC was a kind gift from Lipoid (Ludwigshafen, Germany). POPG and DOPG were purchased from Avanti Polar Lipids (Alabaster, USA). SMA(2:1) hydrolyzed from styrene/maleic anhydride (2:1) (tradename Xiran SZ30010) was provided by Polyscope

(Geleen, Netherlands). DIBMA (Sokalan CP 9) was a kind gift from BASF (Ludwigshafen, Germany). D$_2$O was purchased from Deutero (Kastellaun, Germany), C0mplete (EDTA-free), adenosine triphosphate (ATP), tRNA from *E. coli* MRE 600 and pyruvate kinase (PK) from Roche Diagnostics (Rotkreuz, Switzerland), and formic acid from Honeywell (Morristown, USA). Acetonitrile, chloroacetamide, MS-grade H$_2$O, and NaCl were purchased from VWR (Darmstadt, Germany). 85% w/v H$_3$PO$_4$ in D$_2$O, Na$_2$HPO$_4$, acetyl phosphate (AcP), Mg(OAc)$_2$, KOAc, cytidine triphosphate (CTP), guanosine triphosphate (GTP), uridine triphosphate (UTP) and polyethylene glycol (PEG) 8000 were purchased from Sigma-Aldrich (Steinheim, Germany). Ammonium bicarbonate (ABC), bovine serum albumin (BSA), CaCl$_2$, Coomassie Brilliant Blue G250, dithiothreitol (DTT), ethylenediamine tetraacetic acid (EDTA), folinic acid, 2-(4-(2-hydroxyethyl)-1-piperazinyl)-ethanesulfonic acid (HEPES), MgCl$_2$, NaH$_2$PO$_4$, NaN$_3$, sodium dodecyl sulfate (SDS), sucrose, tris(hydroxymethyl)amino-methane (Tris), Tris-HCl, and amino acids were purchased from Carl Roth (Karlsruhe, Germany). KH$_2$PO$_4$ and phosphoenolpyruvic acid (PEP) were purchased from AppliChem (Darmstadt, Germany), DDM from Glycon (Luckenwalde, Germany), urea from Grüssing (Filsum, Germany), standard polymers (poly(ethylene oxide) (PEO) 24k, Dextran 65k, Dextran 73k, Pullulan 105k) from Malvern Panalytical (Malvern, UK), and RiboLock RNase Inhibitor from Thermo Scientific (Langenselbold, Germany). All chemicals were purchased in the highest purity available.

Synthesis of Sulfo-DIBMA (Poly(diisobutylene-alt-N′,N′-dimethyl(maleimidopropyl)ammonium Propane Sulfonate)): The first step involved the synthesis of poly(diisobutylene-*alt*-N′,N′-dimethylaminopropyl maleimide). 3-(dimethylamino)-1-propylamine (1.08 mL, 8.56 mmol) was added to a solution of DIBMA anhydride (600 mg, 2.85 mmol) in DMF (6 mL). The reaction mixture was stirred at 120 °C for 48 h and then cooled to room temperature. After cooling, the solution was poured into ice-cold water to precipitate the product. The product was collected by centrifugation and dried under vacuum to give a yellowish white solid in quantitative yield. IR (cm^{-1}): 2953 (C−H str), 2873 (C−H str), 1770 (C=O str; cyclic imide), 1700 (C=O str; cyclic imide). Subsequently, poly(diisobutylene-*alt*-N′,N′-dimethylaminopropyl maleimide) (657 mg, 2.23 mmol) was dissolved in CHCl$_3$ (10 mL). To this solution, 1,3-propane sultone (0.59 mL, 6.69 mmol) was added under nitrogen atmosphere at room temperature. The reaction mixture was then stirred overnight at 65 °C, during which the product precipitated. The product was filtered, washed with CHCl$_3$, and dried under vacuum to give Sulfo-DIBMA as a white solid in quantitative yield. IR (cm^{-1}): 2953 (C−H str), 2873 (C−H str), 1767 (C=O str; cyclic imide), 1690 (C=O str; cyclic imide), 1184 (S=O str), 1040 (S=O str).

Synthesis of Sulfo-SMA(2:1) (Poly(styrene-co-N′,N′-dimethyl(maleimidoethyl)ammonium Propane Sulfonate)): The intermediate poly(styrene-co-N′,N′-dimethylaminoethyl maleimide) was synthesized from styrene/maleic anhydride (900 mg, 2.94 mmol) and 2-(dimethylamino)ethylamine (0.96 mL, 8.8 mmol) in a similar manner as for the maleimide intermediate of Sulfo-DIBMA. IR (cm^{-1}): 3084 (=C−H str; aromatic), 2929 (C−H str, aliphatic), 1767 (C=O str; cyclic imide), 1690 (C=O str; cyclic imide). Sulfo-SMA (2:1) was synthesized from poly(styrene-*co*-N′,N′-dimethylaminoethyl maleimide) (400 mg, 1.02 mmol) and 1,3-propane sultone (0.27 mL, 3.07 mmol) in a similar manner as for Sulfo-DIBMA. IR (cm^{-1}): 3084 (=C−H str; aromatic), 2929 (C−H str, aliphatic), 1767 (C=O str; cyclic imide), 1690 (C=O str; cyclic imide), 1184 (S=O str), 1040 (S=O str).

Polymer Stock Solutions: Polymer powders were lyophilized using a Martin Christ Alpha 2–4 LSCplus (Osterode am Harz, Germany) and suspended in either Tris buffer (50 mm Tris, 150 or 200 mm NaCl, pH 7.4 or 8.3) or phosphate buffer (50 mm Na$_2$HPO$_4$/NaH$_2$PO$_4$, 200 mm NaCl, pH 6.5). Samples were then transferred to a preheated ultrasonic bath (Bandelin Sonorex RK 52 H, Berlin, Germany) at 50–70 °C for 15–60 min with vortexing steps in between until the solutions cleared up. Polymer stock solutions were sterile-filtered using 0.45 µm poly(vinylidene fluoride) syringe filters (Carl Roth).

Vesicle Preparation: DMPC or POPG powders were suspended in either Tris buffer (pH 7.4 and 8.3) or phosphate buffer (pH 6.5) to a final lipid concentration of 50–100 mg mL^{-1}. Suspensions were vortexed for 10 min prior to at least 31-fold extrusion through two stacked polycarbonate membranes with a nominal pore diameter of 100 nm. This step was performed at room temperature for DOPG and at 30 °C for DMPC using a block-heated mini-extruder (Avanti, Alabama, USA). Particle-size distributions of large unilamellar vesicles (LUVs) were obtained by DLS (see below), yielding hydrodynamic LUV diameters of ≈120 nm.

Nanodisc Preparation: Samples containing 4 mg mL^{-1} DMPC or POPG—which was added in the form of LUVs—and 0–12 mg mL^{-1} Sulfo-DIBMA or Sulfo-SMA(2:1) in either Tris buffer (pH 7.4 or 8.3) or phosphate buffer (pH 6.5) were incubated for at least 16 h at 30–35 °C (DMPC) or 25 °C (POPG). At polymer/lipid ratios lower than R_{SOL}, the sample contains not only nanodiscs but also partly solubilized vesicles and vesicle aggregates. Within this range of polymer/lipid ratios, particle size is heterogeneous and, therefore, difficult to determine reliably by DLS. Monomodal particle-size distributions can be expected only at ratios above R_{SOL}. In the case of multimodal distributions, the hydrodynamic particle size was taken as the size of the peak corresponding to the smallest particles, which is justified by the steep dependence of light-scattering intensity on particle size. For any method requiring nanodisc dilution (EM, SEC), it should be noted that the concentration of free, nonmembrane-associated polymer will be too low to be detected by most methods.[18] As a practical consequence, nanodisc-containing samples can be diluted using polymer-free buffer without the risk of disrupting the nanodiscs.[4] Although the free forms of Sulfo-DIBMA and Sulfo-SMA(2:1) were impossible to quantitate with the range of methods used in this work, it is safe to assume that the free concentrations of these two electroneutral polymers are at least as low as those of the most hydrophobic polyanionic polymers.

DLS: DLS measurements were carried out on a Zetasizer Nano S90 (Malvern Panalytical, Malvern, UK) equipped with a 633 nm He−Ne laser and a detection angle of 90°. Samples were thermostatted for 2 min at 30–35 °C (DMPC) or 25 °C (POPG) before measurements were performed in a 45-µL quartz glass cuvette with a cross-section of 3 × 3 mm^2 (Hellma Analytics, Müllheim, Germany). Each sample was measured twice: first, with the attenuator position automatically optimized for determination of particle-size distributions and, second, with the attenuator set for optimum total light-scattering intensities. Effects of buffer components and concentrations on the viscosity and refractive index of the solvent were accounted for during data analysis. Autocorrelation functions were fitted by using a non-negatively constrained least-squares function[59] to yield intensity-weighted particle-size distributions, and by cumulant analysis[60] to obtain z-average particle sizes and associated polydispersity indices (PDIs). Distribution widths of z-average sizes, σ, were calculated as $\sigma = \sqrt{PDI}z$.

^{31}P NMR Spectroscopy: Samples containing 2, 4, 6, or 8 mg mL^{-1} DMPC LUVs and 0–24 mg mL^{-1} Sulfo-DIBMA or Sulfo-SMA(2:1) were prepared from stock solutions in Tris buffer at pH 7.4. D$_2$O (10% v/v) was added to the sample buffer to provide a lock signal. NMR measurements were performed at 30 °C on an Avance 600 spectrometer (Bruker Biospin, Rheinstetten, Germany) operating at a 31P resonance of 243 MHz using a 5 mm broadband inverse probe. 128 scans were acquired with an inverse-gated decoupling sequence using an acquisition time of 2.2 s, a sweep width of 7310 Hz, and a relaxation delay of 10 µs. Data were multiplied by an exponential function with a line-broadening factor of 1.0 Hz before Fourier transformation. Chemical shifts were referenced to 85% w/v H$_3$PO$_4$ in D$_2$O as external standard at 0 ppm. Signal peaks were integrated using the software Bruker Topspin 4.0.5.

Negative-Stain TEM: TEM samples were prepared by loading 5 µL polymer-encapsulated nanodiscs with c_l = 5 ng µL^{-1} and m_p/m = 1 onto Quantifoil Cu grids (300 mesh) coated with carbon film (Quantifoil Micro Tools GmbH, Großlöbichau, Germany). Excess liquid was blotted off with a strip of filter paper after 30 s, followed by staining with aqueous uranyl acetate solution (5 µL; 1% w/v). Specimens were dried and examined in an EM 900 transmission electron microscope (Carl Zeiss Microscopy, Oberkochen, Germany), while micrographs were recorded with an SM-1k-120 slow-scan charge-coupled device (SSCCD) camera (TRS, Moorenweis, Germany).

ζ-Potential Measurements: Samples were prepared in low-salt buffer (50 mM Tris, 100 mM NaCl, pH 7.4). Measurements were performed on a Zetasizer Nano ZS (Malvern Panalytical) equipped with a 633 nm He/Ne laser and a backscatter detection angle of 173°. Polymers, nanodiscs, or DMPC LUVs were thermostatted at 35 °C for 2 min before measurements were performed at the same temperature in a folded capillary cell DTS1070 (Malvern Panalytical). A monomodal measurement protocol was used, in which a rapidly alternating electric field is applied, and from which the mean ζ-potential can be derived. The device was calibrated after at least every third new sample by measuring a polystyrene latex standard DTS1235 (Malvern Panalytical) with a ζ-potential of $-(42 \pm 4)$ mV.

DSC: Samples containing DMPC LUVs (4 mg mL^{-1}) and polymer (0–4 mg mL^{-1}) in Tris buffer (pH 7.4) were incubated at 35 °C for 16 h. Sample and reference cells were filled with buffer and repeatedly heated and cooled at a rate of 30 °C h^{-1}. With the exception of the first upscan, successive heating and cooling scans were overlaid very closely. Data were averaged, blank-subtracted, and normalized against the molar amount of DMPC in the sample using the software MicroCal Origin 5.0 (OriginLab, Northampton, USA). The main phase-transition temperature, T_m, was determined as the temperature at which the excess molar isobaric heat capacity, ΔC_p, reached a maximum.

Solubilization of HeLa Membranes: Confluent-grown HeLa cells (cultured in Dulbecco's modified Eagle's medium supplemented with 10% v/v fetal bovine serum, 1% v/v L–glutamine, and 1% v/v penicillin/streptomycin at 37 °C and 5% CO$_2$) were harvested at 4 °C by aspiring the cell medium, followed by two washing steps with phosphate-buffered saline (5 mL; 140 mM NaCl, 2,7 mM KCl, 10 mM Na$_2$HPO$_4$, 1.8 mM KH$_2$PO$_4$) and Tris buffer (5 mL; 150 mM NaCl, pH 7.4) and finally scraping using a sterile cell scraper. Cells were collected, pelleted at 800 g for 10 min, resuspended in 3 mL Tris buffer supplemented with 250 mM sucrose, and homogenized in a precooled Potter–Elvehjem tissue grinder (Corning, New York, USA). The cellular crude extract containing the membranes was ultracentrifuged at 265 000 g for 30 min. The pellet was washed in 3 mL Tris buffer, and the centrifugation step was repeated. To maintain a uniform membrane protein concentration across all experiments, the pellet was weighed and resuspended in an appropriate volume of Tris buffer to achieve a membrane concentration of 60 mg mL^{-1} (wet weight), and was further diluted to 16.7 mg mL^{-1} upon addition of polymer or detergent. Note that membrane fractions were enriched at physiological pH and ion strength without adding detergent prior to polymer addition. After overnight incubation of the solubilization mixture at room temperature on a rotary wheel, samples were ultracentrifuged at 100 000 g and 20 °C for 80 min. Pellets containing insolubilized material were resuspended in Tris buffer containing 2% w/v SDS in equal volumes as supernatant samples containing nanodiscs. Both supernatant and pellet samples were subjected to SDS-PAGE and a BCA (bicinchoninic acid) protein assay.

SDS-PAGE: Protein-extraction yields were determined by SDS-PAGE using a NUPAGE Bis-Tris precast gel with a polyacrylamide gradient of 4–12% (Thermo Fisher Scientific, Schwerte, Germany). Pellet and supernatant samples were diluted with SDS buffer (25 mM DTT, 106 mM Tris-HCl, 141 mM Tris, 2% w/v SDS, 10% w/v glycerol, 0.51 mM EDTA, 0.22 mM Coomassie Brilliant Blue G250, and 0.175 mM Phenol Red, pH 8.5), denatured at 95 °C for 10 min and centrifuged at 10 000 g for 2 min. A voltage of 200 V was applied for 45 min at 50 W. Gels were stained for 60 min in 3.2 mM Coomassie Brilliant Blue R250 in 40% v/v methanol and 10% v/v ethanoic acid, destained for 48 h in water with a paper towel to remove excess Coomassie dye, and photographed.

Multiple-Detection SEC: Mass-average molar masses of Sulfo-DIBMA, Sulfo-SMA(2:1), and the corresponding polymer nanodiscs were determined by SEC on an OmniSEC system (Malvern Panalytical) equipped with a Superose 6 Increase 10/300 GL column (GE Healthcare, Freiburg, Germany) and coupled to UV, static light-scattering, and refractive-index detectors. The column was equilibrated at 30 °C with 3 column volumes (CVs) Tris buffer (pH 7.4) under a steady flow rate of 0.5 mL min^{-1}. 50 µL aliquots of 2.5, 5, 7.5, or 10 mg mL^{-1} polymer and polymer/DMPC nanodiscs with m_p/m_l ranging from 0.5 to 2.0 were injected. Polymer standards (PEO 24k, Dextran 65k, Dextran 73k, and Pullulan 105k, all Malvern Panalytical) were used to generate a calibration curve to estimate mass-average molar masses of lipid-free polymers. Chromatograms of polymer nanodiscs were analyzed with the software OmniSEC v11.0.

SEC of Solubilized Hela Proteins: SEC was carried out on an Äkta Purifier 10 system equipped with a Superose 6 Increase 10/300 GL column and a UV detector (both GE Healthcare) at 8 °C. For Sulfo-DIBMA and Sulfo-SMA(2:1), supernatant samples containing nanodiscs were concentrated using Amicon tubes (Merck, Darmstadt, Germany) with a molar mass cut-off of 10 kDa. The column was equilibrated with 2 CVs precooled Tris buffer (150 mM NaCl, pH 7.4) before 500 µL aliquots of polymer-extracted membrane proteins were injected. 500 µL fractions were collected at a flow rate of 0.3 mL min^{-1}. UV absorbance was recorded at 280 nm for protein detection, 220 nm for DIBMA detection, and 240 nm for Sulfo-DIBMA detection. Collected fractions were lyophilized and stored at −80 °C.

Protein Assay and Precipitation: Lyophilized SEC fractions were resuspended in 110 µL water. To determine the total amount of protein in each fraction, 10 µL of each sample was subjected to a BCA protein assay (Thermo Fisher Scientific)[61] performed on a FLUOstar Omega plate reader (BMG Labtech, Ortenberg, Germany). Proteins in the remaining 100 µL were precipitated using a modified variant of a published chloroform/methanol precipitation procedure.[62] Briefly, methanol (400 µL) was added to ice-cold sample (100 µL), and the mixture was vortexed for 3 s. Chloroform (200 µL) was added, the mixture was vortexed again for 3 s, and water (300 µL) was added. The sample was vortexed thoroughly for 10 s and centrifuged at 14 000 g for 3 min in a precooled centrifuge at 4 °C. The upper aqueous phase was removed before addition of another 400 µL of methanol, vortexing for 15 s, and centrifugation at 5000 g and 20 000 g for 1 and 4 min, respectively. The supernatant was discarded, and the protein pellet was dried either in a vacuum desiccator (DWK Life Sciences, Wertheim, Germany) at room temperature overnight or in a Jouan RC1010 vacuum concentrator (Thermo Fisher Scientific) at 40 °C for 45 min.

In-Solution Digest and Sample Clean-Up: Precipitated SEC fractions were resuspended in denaturing ABC buffer (25 µL; 8 M urea, 25 mM ammonium bicarbonate). 1,4-Dithiothreitol and chloroacetamide were added separately to final concentrations of 12.5 and 25 mM, respectively, and the sample was incubated for 30 min. Samples were diluted with ABC buffer (25 mM ammonium bicarbonate) to 4 M urea, Lys-C was added to reach a final Lys-C/protein mass ratio of 1:100, and the mixture was incubated at 37 °C for at least 3 h. After the initial digest, the sample was further diluted with ABC buffer to 1 M urea, acetonitrile and trypsin were added to reach a final concentration of 5% v/v and a trypsin/protein mass ratio of 1:100, respectively, and the mixture was incubated at 37 °C for at least 12 h. An additional digest was performed by adding trypsin to give a final trypsin/protein mass ratio of 1:50, followed by another incubation at 37 °C for 3 h. Samples were acidified by adding formic acid to give a final concentration of 2% v/v. Sample clean-up was performed following a modified version of a previously published protocol for peptide desalting (STAGE tipping).[63] To this end, peptide desalting spin columns were prepared with two layers of Empore C18 filter extraction discs and equilibrated with ABC (25 mM) and formic acid (0.1% v/v), which was also used for column washing after sample loading. Peptides were then eluted by pushing ABC 25 mM, acetonitrile (80% v/v), formic acid (0.1% v/v) through the tips. The eluate was dried in a RVC 2-25 CD plus vacuum concentrator (Martin Christ, Osterode am Harz, Germany) at 30 mbar and 40 °C for 60 min, and then subjected to mass spectrometry.

MS: Protein identification and quantification were performed on an Easy-nLC 1200 HPLC coupled to a Q Exactive HF mass spectrometer (Thermo Fisher Scientific). Peptides were separated on reversed-phase columns (30 cm long with an inner diameter of 75 µm; New Objective, Woburn, MA) packed in-house with ReproSil-Pur 120 C18-AQ (Dr. Maisch, Ammerbruch-Entrigen, Germany) using buffer A (0.1% v/v formic acid) and buffer B (80% v/v acetonitrile, 0.1% v/v formic acid) as mobile phases. Eluting peptides were directly injected into the mass

spectrometer. Dried peptides of each fraction were resuspended in 5 μL 2% v/v acetonitrile and 0.1% v/v formic acid in MS-grade H_2O. 4 μL of each fraction was separated on the C18 column using a 90 min gradient from 5% to 95% (v/v) buffer B. The following LC gradient steps were used: 00:00 min: 2% B; 05:00 min: 5% B; 65:00 min: 30% B; 70:00 min: 60% B; 75:00 min: 95% B; 80:00 min: 95% B; 85:00 min: 2% B; 90:00 min: 2% B.

MS data were analyzed with MaxQuant (version 2.0.1.0).[64] A false-discovery rate (FDR) of 0.01 for peptides and a minimum peptide length of 7 amino acid residues were required. For Andromeda search, trypsin allowing for cleavage N-terminal of proline was chosen as enzyme specificity. Cysteine carbamidomethylation was selected as a fixed modification, and protein N-terminal acetylation and methionine oxidation were selected as variable modifications. A maximum of two missed cleavages was allowed. Initial mass deviation of precursor ion was limited to 7 ppm and mass deviation for fragment ions to 0.5 Da. Protein identification required at least one unique in each protein group. "Match between run" was used to transfer identities within all replicate samples of the unfractionated samples and between adjacent SEC fractions. For data analysis, an Excel spreadsheet and the Solver add-in were used for nonlinear least-squares fitting.[65] MS data matrices were processed with the MaxQuant companion software Perseus.[66] Comparison against other proteome-profiling studies was done using the Gene Ontology cell compartment keyword "membrane."[67]

MDS: MDS measurements with postseparation labeling[30,68] using injection-molded disposable plastic chips were performed on a Fluidity One instrument (Fluidic Analytics, Cambridge, UK). Protein/Peptide concentrations were 5/25/25 μm for α-synuclein/ACTH/GB1, respectively. Lipid concentrations, as determined via Fourier-transform IR, for either DMPC or DMPG discs were 0.125/2.5/25 mm for interaction studies with α-synuclein/ACTH/GB1, respectively.[31] α-synuclein was produced as described previously.[36] ACTH was produced in *E. coli* using a GB1 fusion construct containing an N-terminal hexahistidine tag and a C-terminal TEV recognition site. After immobilized metal affinity chromatography (IMAC), the solubility tag was removed using TEV protease followed by a second IMAC step resulting in pure wild-type ACTH and the residual GB1 construct.

Nanodisc Assembly for Cell-Free Protein Translation: DOPG was used for nanodisc formation because it has previously been found to perform best on the selected membrane proteins with MSP nanodiscs.[43] DOPG LUVs extruded to 200 nm and polymer stock solutions (50 mm Tris, 150 mm NaCl, pH 7.4) were mixed in various polymer/lipid mass ratios ($m_{polymer}/m_{DOPG}$ = 1.3, 2.6, 5.2, or 10.3) and incubated at room temperature for 24 h. Nanodisc formation was monitored by observing clearance of the turbid solution. Subsequently, the mixtures were centrifuged at 20000 g to remove larger aggregates. Supernatants were concentrated using Amicon tubes (Merck, Darmstadt, Germany) with a 10-kDa cut-off. To monitor the size of the polymer nanodiscs, SEC was carried out at 12 °C using a Superdex 200 Increase 3.2/300 GL column connected to an Äkta purifier system (both GE Healthcare, Freiburg, Germany). Prior to injecting the nanodisc samples, the column was equilibrated in pre-cooled buffer (50 mm Tris, 150 mm NaCl, pH 7.4). Chromatography was conducted at a flow rate of 0.05 mL min^{-1}, and UV absorbance was recorded at 240 nm. This was to screen the nanodiscs formed at the above-mentioned polymer/DOPG mass ratios for their suitability in supporting cell-free membrane-protein production. For both Sulfo-DIBMA and Sulfo-SMA(2:1), SEC showed that maximum sample homogeneity was achieved at a polymer/DOPG mass ratio of 2.6, which was thus used for the following experiments.

Cell-Free Protein Translation: Cell-free translation was carried out as described in detail previously.[43,45] Briefly, S30 lysates were prepared from *E. coli* A19 strain. Analytical-scale reactions were performed in 55 μL reaction mixtures (RM) separated from feeding mixtures (FM) with dialysis membranes with a molecular weight cut-off of 12–14 kDa (Carl Roth). The volume ratio of RM to FM was 1:15. For membrane-protein synthesis and membrane insertion, preformed polymer nanodiscs were added into the RM in final concentrations of 30–240 μm. Reactions were

incubated at 30 °C for 16–20 h with shaking. After translation, RMs were collected and centrifuged at 18000 g and 4 °C for 10 min to remove aggregates.

SEC of Proteorhodopsin Synthesized in a Cell-Free Manner: Proteorhodopsin production was quantified by measuring its specific UV absorbance at 530 nm directly in the cell-free reaction. After translation, proteorhodopsin was purified via a C-terminal strep-tag. The proteorhodopsin solution was diluted 1:3 in buffer A (100 mm Tris, 100 mm NaCl, pH 8.0), loaded and reloaded twice on a Strep column pre-equilibrated with the same buffer. The column was washed with 10 CV buffer and proteorhodopsin was eluted using buffer supplemented with 25 mm D-desthiobiotin (Sigma-Aldrich, Steinheim, Germany). The purified protein was concentrated in Amicon tubes (Merck, Darmstadt, Germany) with a 10-kDa cut-off and centrifuged at 20 000 g and 4 °C for 10 min before injection onto the SEC column. SEC was carried out at 12 °C using a Superose 6 10/300 GL column connected to an Äkta purifier system (GE Healthcare, Freiburg, Germany). The column was equilibrated in precooled buffer A before the proteorhodopsin sample was injected. The run was conducted at a flow rate of 0.3 mL min^{-1}, and UV absorbance was recorded at 280 nm.

Radioligand Filter Binding Assay: The Tβ1AR construct was modified by fusing GFP to its C-terminal end.[45] Final concentrations of 10 nm Tβ1AR and 50 nm [^{3}H]dihydroalprenolol (Biotrend, Köln, Germany) were incubated in 30 μL aliquots of binding buffer (50 mm HEPES, pH 7.5, 1 mm, CaCl$_2$, 5 mm MgCl$_2$, 0.2% w/v BSA) for 1 h at room temperature with gentle shaking. Unspecific binding was determined by preincubating the samples with 40 μm nonlabeled alprenolol (Torcis, Bristol, UK) for 1 h before adding [^{3}H]dihydroalprenolol. GF/B glass-fiber filters (Merck, Darmstadt, Germany) were pretreated with polyethyleneimine (0.3% w/v) for 30 min and washed 5 times with filter-wash buffer (150 μL; 50 mm HEPES, pH 7.5, 0.5% w/v BSA). Samples were transferred to glass-fiber filters and subsequently washed 7 times with high-salt buffer (150 μL; 50 mm HEPES, pH 7.5, 500 mm NaCl, 0.1% w/v BSA)). Filters were submerged in Rotiszint eco plus (2 mL; Carl Roth), and radioactivity was measured on a Hidex 300 SL liquid scintillation counter (Hidex, Turku, Finland).

Supporting Information

Supporting Information is available from the Wiley Online Library or from the author.

Acknowledgements

Conflict of Interest

The authors declare no conflict of interest.

Data Availability Statement

MS proteomics data and acquisition parameters were deposited in the ProteomeXchange Consortium via the PRIDE partner repository with the dataset identifier PXD030958.

Keywords

[1] R. Santos, O. Ursu, A. Gaulton, A. P. Bento, R. S. Donadi, C. G. Bologa, A. Karlsson, B. Al-Lazikani, A. Hersey, T. I. Oprea, J. P. Overington, *Nat. Rev. Drug. Discovery* **2017**, *16*, 19.

[2] F. Mahler, A. Meister, C. Vargas, G. Durand, S. Keller, *Small* **2021**, *17*, e2103603.

[3] T. H. Bayburt, Y. V. Grinkova, S. G. Sligar, *Nano Lett.* **2002**, *2*, 853.

[4] S. C. Lee, T. J. Knowles, V. L. G. Postis, M. Jamshad, R. A. Parslow, Y.-P. Lin, A. Goldman, P. Sridhar, M. Overduin, S. P. Muench, T. R. Dafforn, *Nat. Protoc.* **2016**, *11*, 1149.

[5] A. O. Oluwole, B. Danielczak, A. Meister, J. O. Babalola, C. Vargas, S. Keller, *Angew. Chem., Int. Ed.* **2017**, *56*, 1919.

[6] S. Tonge, B. Tighe, *Adv. Drug Delivery Rev.* **2001**, *53*, 109.

[7] A. A. Smith, H. E. Autzen, B. Faust, J. L. Mann, B. W. Muir, S. Howard, A. Postma, A. J. Spakowitz, Y. Cheng, E. A. Appel, *Chem* **2020**, *6*, 2782.

[8] H. J. Lee, H. S. Lee, T. Youn, B. Byrne, P. S. Chae, *Chem* **2022**, *13*, 5750.

[9] T. J. Knowles, R. Finka, C. Smith, Y.-P. Lin, T. Dafforn, M. Overduin, *J. Am. Chem. Soc.* **2009**, *131*, 7484.

[10] J. M. Dörr, S. Scheidelaar, M. C. Koorengevel, J. J. Dominguez, M. Schäfer, C. A. van Walree, J. A. Killian, *Eur. Biophys. J.* **2016**, *45*, 3.

[11] A. Olerinyova, A. Sonn-Segev, J. Gault, C. Eichmann, J. Schimpf, A. H. Kopf, L. S. P. Rudden, D. Ashkinadze, R. Bomba, L. Frey, J. Greenwald, M. T. Degiacomi, R. Steinhilper, J. A. Killian, T. Friedrich, R. Riek, W. B. Struwe, P. Kukura, *Chem* **2021**, *7*, 224.

[12] A. M. Seddon, P. Curnow, P. J. Booth, *Biochim. Biophys. Acta* **2004**, *1666*, 105.

[13] N. L. Pollock, J. Lloyd, C. Montinaro, M. Rai, T. R. Dafforn, *Biochem. J.* **2022**, *479*, 145.

[14] V. M. Luna, M. Vazir, A. Vaish, S. Chong, I. Chen, H. K. Yamane, *Eur. Polym. J.* **2018**, *109*, 483.

[15] M. C. Fiori, Y. Jiang, G. A. Altenberg, H. Liang, *Sci. Rep.* **2017**, *7*, 7432.

[16] M. C. Fiori, W. Zheng, E. Kamilar, G. Simiyu, G. A. Altenberg, H. Liang, *Sci. Rep.* **2020**, *10*, 9940.

[17] T. Ravula, N. Z. Hardin, S. K. Ramadugu, A. Ramamoorthy, *Langmuir* **2017**, *33*, 10655.

[18] K. Janson, J. Zierath, F. L. Kyrilis, D. A. Semchonok, F. Hamdi, I. Skalidis, A. H. Kopf, M. Das, C. Kolar, M. Rasche, C. Vargas, S. Keller, P. L. Kastritis, A. Meister, *Biochim. Biophys. Acta Biomembr.* **2021**, *1863*, 183725.

[19] A. O. Oluwole, J. Klingler, B. Danielczak, J. O. Babalola, C. Vargas, G. Pabst, S. Keller, *Langmuir* **2017**, *33*, 14378.

[20] S. C. L. Hall, C. Tognoloni, J. Charlton, É. C. Bragginton, A. J. Rothnie, P. Sridhar, M. Wheatley, T. J. Knowles, T. Arnold, K. J. Edler, T. R. Dafforn, *Nanoscale* **2018**, *10*, 10609.

[21] A. Grethen, A. O. Oluwole, B. Danielczak, C. Vargas, S. Keller, *Sci. Rep.* **2017**, *7*, 11517.

[22] A. W. Shaw, M. A. McLean, S. G. Sligar, *FEBS Lett.* **2004**, *556*, 260.

[23] M. Jamshad, V. Grimard, I. Idini, T. J. Knowles, M. R. Dowle, N. Schofield, P. Sridhar, Y.-P. Lin, R. Finka, M. Wheatley, O. R. Thomas, R. E. Palmer, M. Overduin, C. Govaerts, J.-M. Ruysschaert, K. J. Edler, T. R. Dafforn, *Nano Res.* **2015**, *8*, 774.

[24] E. Freire, R. Biltonen, *Biochim. Biophys. Acta Biomembr.* **1978**, *514*, 54.

[25] S. Scheidelaar, M. C. Koorengevel, J. D. Pardo, J. D. Meeldijk, E. Breukink, J. A. Killian, *Biophys. J.* **2015**, *108*, 279.

[26] H. A. Lashuel, C. R. Overk, A. Oueslati, E. Masliah, *Nat. Rev. Neurosci.* **2013**, *14*, 38.

[27] H. Gang, C. Galvagnion, G. Meisl, T. Müller, M. Pfammatter, A. K. Buell, A. Levin, C. M. Dobson, B. Mu, T. P. J. Knowles, *Anal. Chem.* **2018**, *90*, 3284.

[28] L. Macikova, V. Sinica, A. Kadkova, S. Villette, A. Ciaccafava, J. Faherty, S. Lecomte, I. D. Alves, V. Vlachova, *FEBS J.* **2019**, *286*, 3664.

[29] M. Azouz, M. Gonin, S. Fiedler, J. Faherty, M. Decossas, C. Cullin, S. Villette, M. Lafleur, I. D Alves, S. Lecomte, A. Ciaccafava, *Biochim. Biophys. Acta Biomembr.* **2020**, *1862*, 183215.

[30] P. Arosio, T. Müller, L. Rajah, E. V. Yates, F. A. Aprile, Y. Zhang, S. I. A. Cohen, D. A. White, T. W. Herling, E. J. d. Genst, S. Linse, M. Vendruscolo, C. M. Dobson, T. P. J. Knowles, *ACS Nano* **2016**, *10*, 333.

[31] M. Falke, J. Victor, M. M. Wördehoff, A. Peduzzo, T. Zhang, G. F. Schröder, A. K. Buell, W. Hoyer, M. Etzkorn, *Chem. Phys. Lipids.* **2019**, *220*, 57.

[32] D. Sulzer, R. H. Edwards, *J. Neurochem.* **2019**, *150*, 475.

[33] B. D. van Rooijen, M. M. A. E. Claessens, V. Subramaniam, *Biochim. Biophys. Acta* **2009**, *1788*, 1271.

[34] G. Fusco, A. d. Simone, T. Gopinath, V. Vostrikov, M. Vendruscolo, C. M. Dobson, G. Veglia, *Nat. Commun.* **2014**, *5*, 3827.

[35] L. Fonseca-Ornelas, S. E. Eisbach, M. Paulat, K. Giller, C. O. Fernández, T. F. Outeiro, S. Becker, M. Zweckstetter, *Nat. Commun.* **2014**, *5*, 5857.

[36] T. Viennet, M. M. Wördehoff, B. Uluca, C. Poojari, H. Shaykhalishahi, D. Willbold, B. Strodel, H. Heise, A. K. Buell, W. Hoyer, M. Etzkorn, *Commun. Biol.* **2018**, *1*, 44.

[37] P. Verhallen, R. A. Demel, H. Zwiers, W. H. Gispen, *Biochim. Biophys. Acta Biomembr.* **1984**, *775*, 246.

[38] A. Stevens, A. White, *Results. Probl. Cell. Differ.* **2010**, *50*, 63.

[39] Z. Zhang, T. J. Melia, F. He, C. Yuan, A. McGough, M. F. Schmid, T. G. Wensel, *J. Biol. Chem.* **2004**, *279*, 33937.

[40] T. S. Ulmer, A. Bax, N. B. Cole, R. L. Nussbaum, *J. Biol. Chem.* **2005**, *280*, 9595.

[41] A. D. Silverman, A. S. Karim, M. C. Jewett, *Nat. Rev. Genet.* **2020**, *21*, 151.

[42] M. L. Shelby, W. He, A. T. Dang, T. L. Kuhl, M. A. Coleman, *Front. Pharmacol.* **2019**, *10*, 744.

[43] R.-B. Rues, A. Gräwe, E. Henrich, F. Bernhard, *Methods Mol. Biol.* **2017**, *1586*, 291.

[44] E. Henrich, O. Peetz, C. Hein, A. Laguerre, B. Hoffmann, J. Hoffmann, V. Dötsch, F. Bernhard, N. Morgner, *Elife* **2017**, *6*, e20954.

[45] R.-B. Rues, V. Dötsch, F. Bernhard, *Biochim. Biophys. Acta* **2016**, *1858*, 1306.

[46] N. Nagaraj, J. R. Wisniewski, T. Geiger, J. Cox, M. Kircher, J. Kelso, S. Pääbo, M. Mann, *Mol. Syst. Biol.* **2011**, *7*, 548.

[47] T. Robin, A. Bairoch, M. Müller, F. Lisacek, L. Lane, *J. Proteome Res.* **2019**, *18*, 1926.

[48] A. Erfani, J. Seaberg, C. P. Aichele, J. D. Ramsey, *Biomacromolecules* **2020**, *21*, 2557.

[49] M. Wang, D. L. Roberts, R. Paschke, T. M. Shea, B. S. Masters, J. J. Kim, *Proc. Natl. Acad. Sci. USA* **1997**, *94*, 8411.

[50] E. Prade, M. Mahajan, S.-C. Im, M. Zhang, K. A. Gentry, G. M. Anantharamaiah, L. Waskell, A. Ramamoorthy, *Angew. Chem., Int. Ed.* **2018**, *57*, 8458.

[51] R. Slaaby, L. Schäffer, I. Lautrup-Larsen, A. S. Andersen, A. C. Shaw, I. S. Mathiasen, J. Brandt, *J. Biol. Chem.* **2006**, *281*, 25869.

[52] M. Bublitz, J. P. Morth, P. Nissen, *J. Cell. Sci.* **2011**, *124*, 2515.

[53] M. Heusel, I. Bludau, G. Rosenberger, R. Hafen, M. Frank, A. Banaei-Esfahani, A. van Drogen, B. C. Collins, M. Gstaiger, R. Aebersold, *Mol. Syst. Biol.* **2019**, *15*, e8438.

[54] A. Magri, A. Messina, *Curr. Med. Chem.* **2017**, *24*, 4470.

[55] A. Boulbrima, D. Temple, G. Psakis, *Biochem. Soc. Trans.* **2016**, *44*, 1531.

[56] M. T. Marty, K. C. Wilcox, W. L. Klein, S. G. Sligar, *Anal. Bioanal. Chem.* **2013**, *405*, 4009.

[57] A. J. Keefe, S. Jiang, *Nat. Chem.* **2011**, *4*, 59.

[58] S. Fiedler, M. A. Piziorska, V. Denninger, A. S. Morgunov, A. Ilsley, A. Y. Malik, M. M. Schneider, S. R. A. Devenish, G. Meisl, V. Kosmoliaptsis, A. Aguzzi, H. Fiegler, T. P. J. Knowles, *ACS Infect. Dis.* **2021**, *7*, 2362.

[59] P. A. Hassan, S. Rana, G. Verma, *Langmuir* **2015**, *31*, 3.

[60] D. E. Koppel, *J. Chem. Phys.* **1972**, *57*, 4814.

[61] P. K. Smith, R. I. Krohn, G. T. Hermanson, A. K. Mallia, F. H. Gartner, M. D. Provenzano, E. K. Fujimoto, N. M. Goeke, B. J. Olson, D. C. Klenk, *Anal. Biochem.* **1985**, *150*, 76.

[62] D. Wessel, U. I. Flügge, *Anal. Biochem.* **1984**, *138*, 141.

[63] J. Rappsilber, M. Mann, Y. Ishihama, *Nat. Protoc.* **2007**, *2*, 1896.

[64] J. Cox, M. Mann, *Nat. Biotechnol.* **2008**, *26*, 1367.

[65] G. Kemmer, S. Keller, *Nat. Protoc.* **2010**, *5*, 267.

[66] S. Tyanova, T. Temu, P. Sinitcyn, A. Carlson, M. Y. Hein, T. Geiger, M. Mann, J. Cox, *Nat. Methods* **2016**, *13*, 731.

[67] M. Ashburner, C. A. Ball, J. A. Blake, D. Botstein, H. Butler, J. M. Cherry, A. P. Davis, K. Dolinski, S. S. Dwight, J. T. Eppig, M. A. Harris, D. P. Hill, L. Issel-Tarver, A. Kasarskis, S. Lewis, J. C. Matese, J. E. Richardson, M. Ringwald, G. M. Rubin, G. Sherlock, *Nat. Genet.* **2000**, *25*, 25.

[68] E. V. Yates, T. Müller, L. Rajah, E. J. d. Genst, P. Arosio, S. Linse, M. Vendruscolo, C. M. Dobson, T. P. J. Knowles, *Nat. Chem.* **2015**, *7*, 802.